Dark matter limits from dwarf satellites

Piero Ullio

SISSA, IFPU & INFN Trieste

Cosmology 2018 in Dubrovnik, October 23, 2018

Milky Way dwarfs at the forefront in indirect DM searches

Prompt GeV-TeV photon emission in DM pair annihilations, as one of the most promising indirect detection channels:

$$\frac{d\Phi_\gamma}{dE_\gamma} = \frac{1}{4\pi} \frac{(\overline{\sigma v}_{\rm rel})}{2m_\chi^2} \frac{dN_\gamma}{dE_\gamma} \cdot J(\psi, \Delta\Omega)$$

"particle physics" term

"astrophysics" term: ~ l.o.s. + detector angular acceptance integrals of the square of the DM density in a given target

Recent null searches (tentative GC detection) from Fermi LAT:

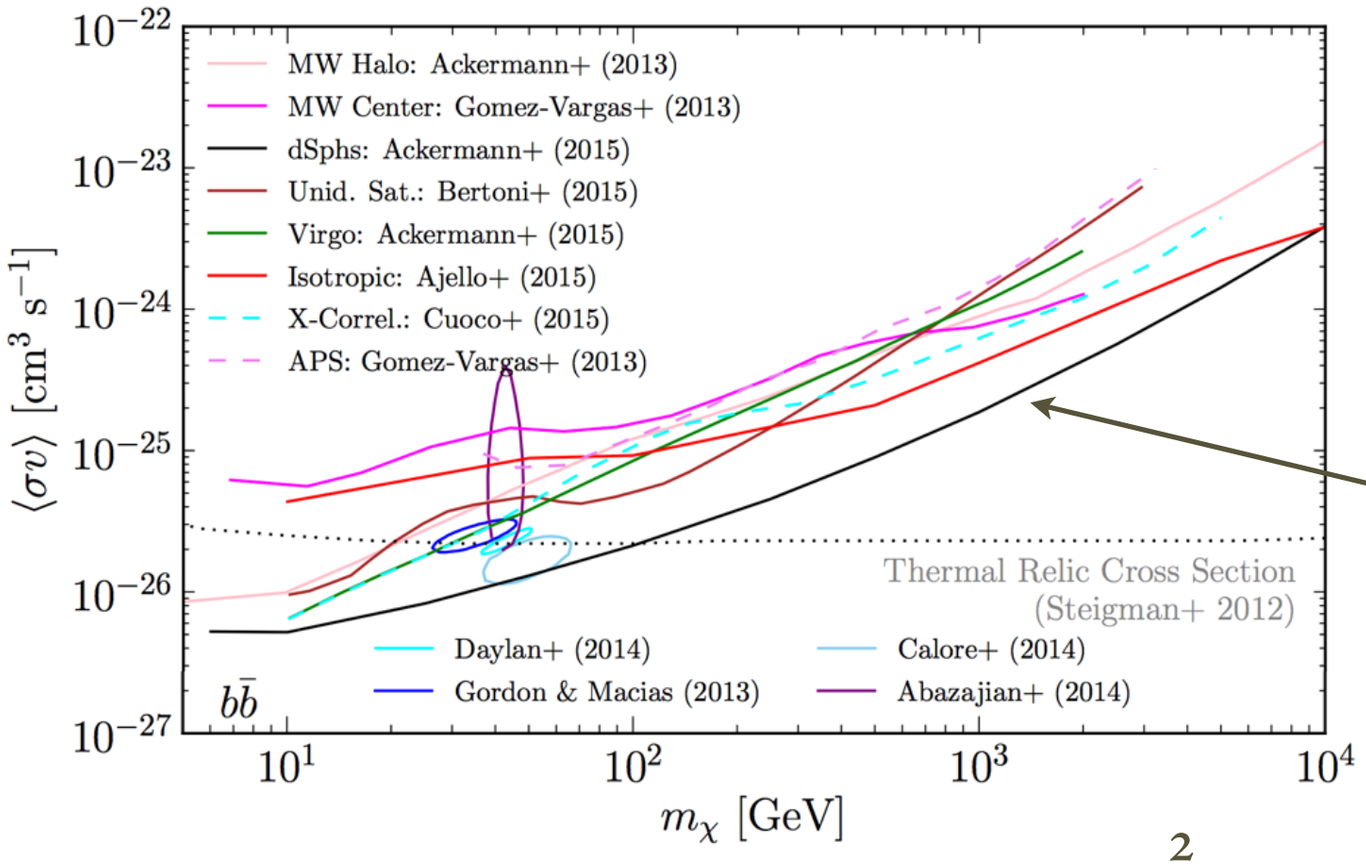

Charles et al., 2016

Tightest limit from MW dwarf satellites, **Fermi Coll. 2015**. Thermal relic WIMPs lighter than ~100 GeV excluded (???)

Milky Way dwarfs as Dark Matter detection Labs

Ideal targets for **detecting** a DM signal (prompt or radiative emission from DM particle pair annihilations or decays):

- objects with fairly large DM densities, located fairly close to the Sun (about 10 to 200 kpc);

- intrinsic backgrounds from "standard" astrophysical sources below detection sensitivities (?)
+ low Milky Way foregrounds (intermediate to high latitude locations).

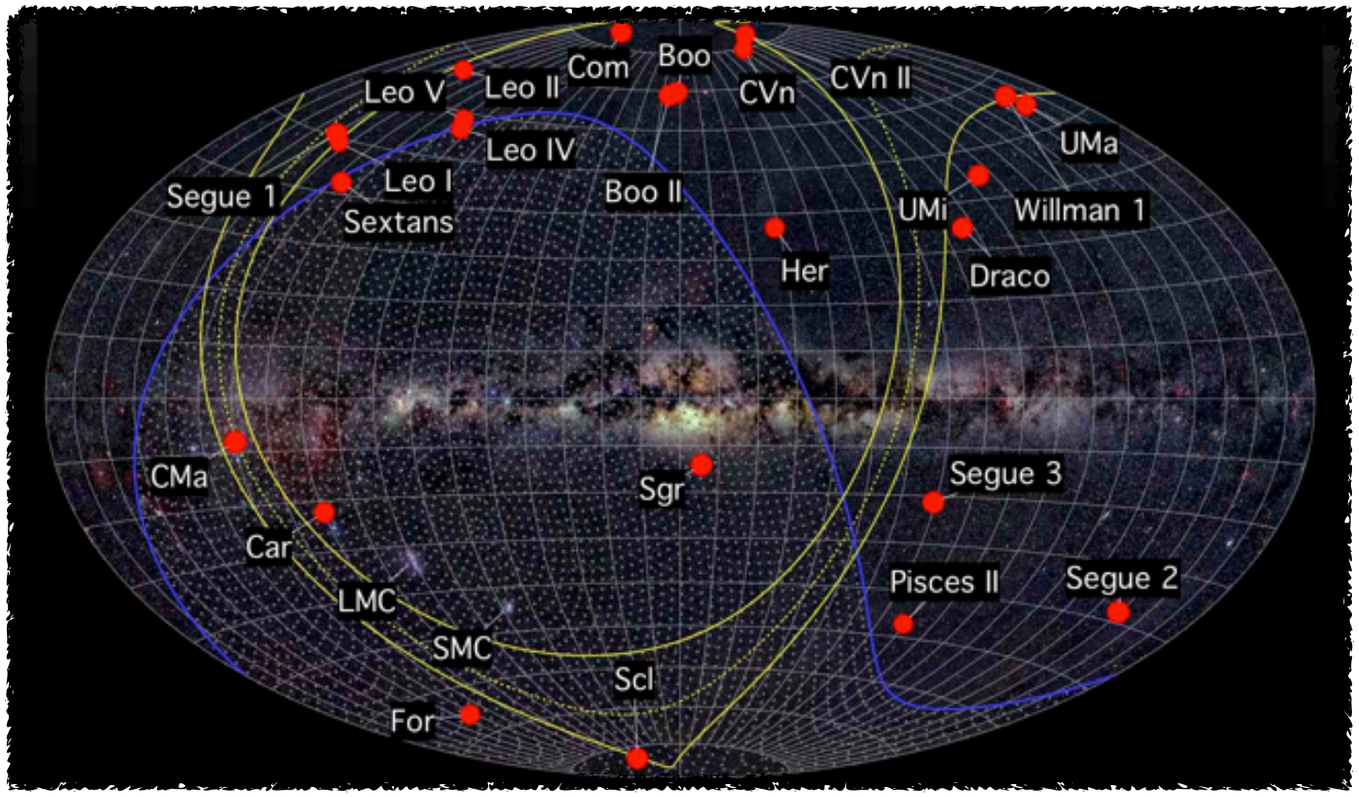

Over 50 (spectroscopically) identified;
8 with adequate kinematic data samples,
the so-called "classical" dwarfs.

Are they ideal targets for **setting limits** as well? For the classical dwarfs 1-σ uncertainties on J-factors often assumed within factors of 1.5 « the "astro" uncertainty in any other indirect detection tool! Where does it come from?

Mass models for dwarf galaxies

A stellar population as tracer of the gravitational potential (i.e. the DM distribution) assuming dynamical equilibrium. Velocity moments of the collision-less Boltzmann equation. Spherical symmetry for all components:

$\Rightarrow$ a single Jeans equation

$$\frac{d}{dr}\left(\nu_\star \sigma^2_{rr,\star}\right) + \frac{2\beta_\star(r)}{r}\nu_\star\sigma^2_{rr,\star} = -\nu_\star\frac{M(r)}{r^2}.$$

Usually solved for the stellar radial pressure: $p_\star(r) \equiv \nu_\star(r)\sigma^2_{rr,\star}(r)$ in terms of the 3 unknown functions:

the star density profile	the star anisotropy profile	the DM mass profile
$\nu_\star(r)$	$\beta_\star(r) = 1 - \frac{\sigma^2_{\varphi\varphi,\star} + \sigma^2_{\theta\theta,\star}}{2\sigma^2_{rr,\star}}$	$M(r)$

$$-\infty \leq \beta_\star(r) \leq 1$$

circular orbits

radial orbits

isotropy: $\beta_\star(r) = 0$

Mass models for dwarf galaxies (ii)

The 3 unknowns: $\nu_\star(r)$, $\beta_\star(r)$ and $M(r)$ can be mapped into 2 observables:

the star surface brightness

$$I_\star(R) = \int_R^\infty dr \frac{2r}{\sqrt{r^2 - R^2}} \nu_\star(r)$$

the l.o.s. velocity dispersion

$$\sigma^2_{los}(R) = \frac{1}{I_\star(R)} \int_R^\infty dr \frac{2r}{\sqrt{r^2 - R^2}} \left[1 - \beta_\star(r) \frac{R^2}{r^2}\right] p_\star(r)$$

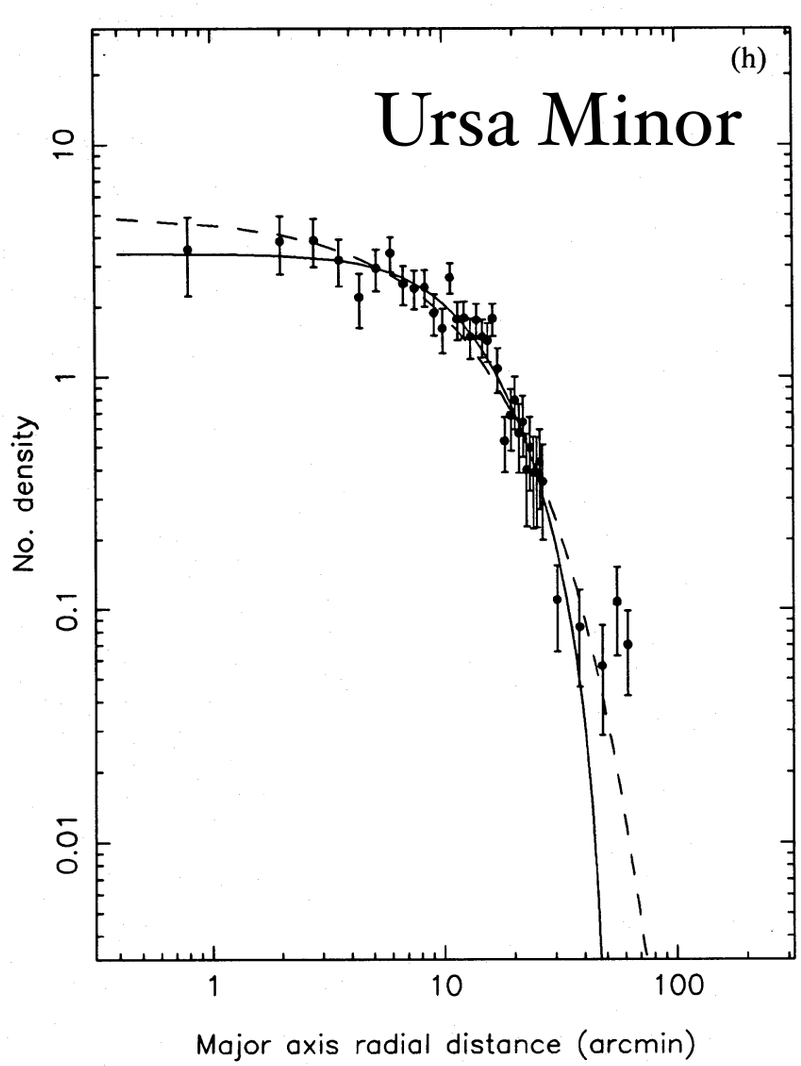

Irwin + Hatzidimitriuo 1995

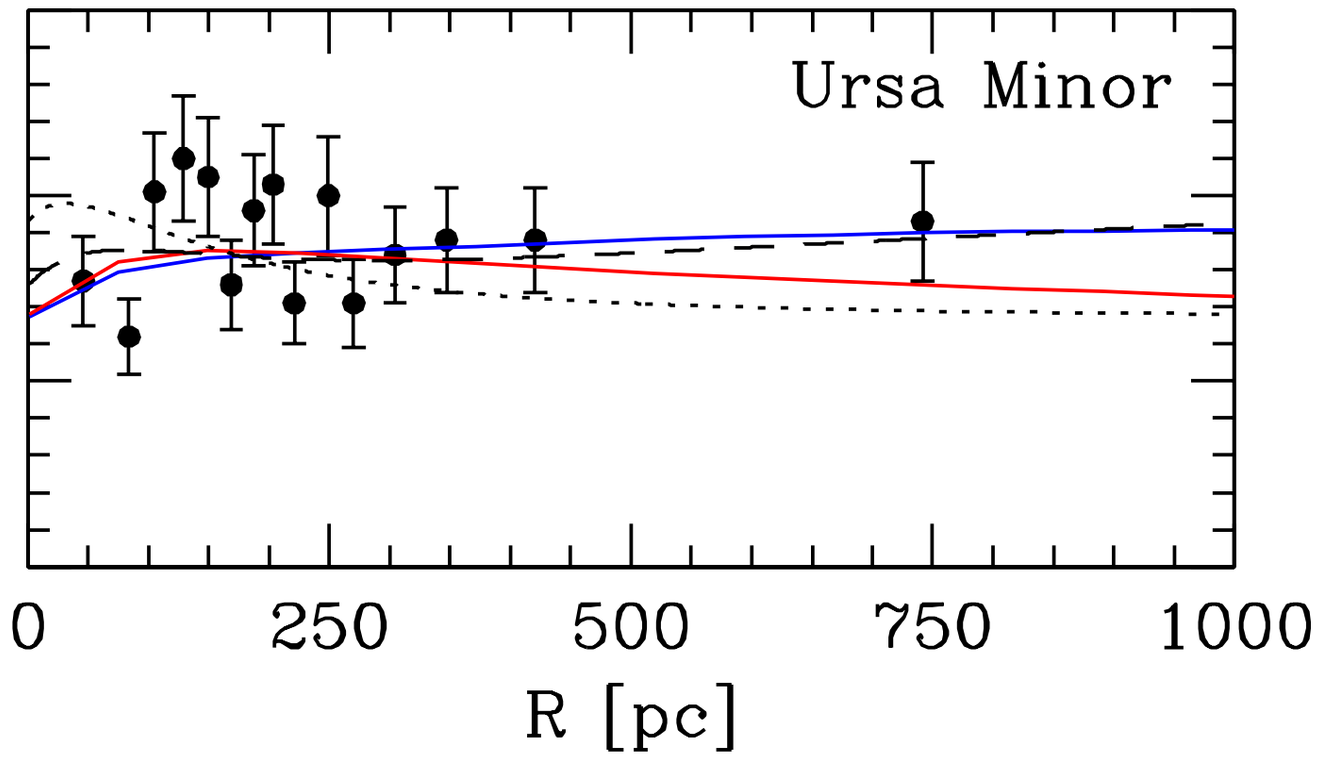

e.g.: **Walker et al. 2009**

Mass models for dwarf galaxies (iii)

The mapping is usually done introducing parametric forms for:

$\nu_\star(r)$ - Plummer, King, Sersic ... profile as supported from star profiles in other observed systems;

$M(r)$ [or DM $\rho(r)$] - from N-body simulations or DM phenomenology;

$\beta_\star(r)$ - as an arbitrary choice, since there is no real observational handle.

and performing:

- a frequentist fit of $\nu_\star(r)$ to data on $I_\star(R)$;

- Bayesian inference from the stellar kinematics comparing predicted and measured $\sigma^2_{l.o.s.}(R)$, addressing the large parameter space with a MCMC sampling of a properly defined likelihood; delicate choice for parameter priors, again arbitrary for $\beta_\star(r)$. Posteriors on $M(r)$ [or DM $\rho(r)$] after marginalization over parameters. The derived posterior for J (and its small error bar) is what will enter as an input for particle physics limits.

Is this a fully reliable approach?

A recent update following this mass modelling recipe:

Stellar profiles modelled via a Plummer model (***1-parameter***):

$$I_\star(R) \propto \left(1+(R/R_{1/2})^2\right)^{-2} \quad \Leftrightarrow \quad \nu_\star(r) \propto 3/(4R_{1/2})\left(1+(R/R_{1/2})^2\right)^{-5/2}$$

The dark matter profile in two alternative ***2-parameter*** forms:

NFW: $\rho_{\rm NFW} = \dfrac{\rho_s}{(r/r_s)\,(1+r/r_s)^2}$ Burkert: $\rho_{\rm BUR} = \dfrac{\rho_s}{(1+r/r_s)\,(1+(r/r_s)^2)}$

The stellar anisotropy profile in a rather generic form interpolating between its value at small radii β_0 and the one in the outskirts β_∞:

$$\beta_\star(r) = \frac{\beta_0 + \beta_\infty (r/r_\beta)^2}{1+(r/r_\beta)^2} \qquad (\textbf{\textit{3-parameter}} \text{ form})$$

In total a setup with ***7 parameters***:

$$\vec{\theta} = \{\rho_s, r_s, r_\beta, \beta_0, \beta_\infty, \alpha_{1/2}, D\}$$

having included the heliocentric distance of the object D among the quantities to sample, and introduced $\alpha_{1/2} = D/R_{1/2}$.

A recent update following this mass modelling recipe (ii):

A MCMC fitting procedure exploiting Bayes' theorem:

$$\mathcal{P}\left(\vec{\theta} \mid \text{data}\right) \propto \mathcal{P}_0\left(\vec{\theta}\right) \mathcal{L}_{\text{tot}}\left(\text{data} \mid \vec{\theta}\right)$$

specifying a likelihood, which, for the part connected to measured stellar kinematics in MW satellites, reads:

$$\mathcal{L}_{\text{kin}} \equiv \prod_{k=1}^{\text{N}} \frac{1}{\sqrt{2\pi}\,\Delta\sigma_{los\,(k)}\left(\alpha_{(k)}\right)} \exp\left[-\frac{1}{2}\left(\frac{\overline{\sigma}_{los\,(k)} - \sigma_{los}\left(\alpha_{(k)}\right)}{\Delta\sigma_{los\,(k)}\left(\alpha_{(k)}\right)}\right)^2\right]$$

($\overline{\sigma}_{los\,(k)}$ is the measured value in the k angular bin, $\sigma_{los}\left(\alpha_{(k)}\right)$ is the predicted value according to the solution of the spherical Jeans equation at the center of the bin, the error $\Delta\sigma_{los\,(k)}$ takes into account the binning)

and a set of priors:

flat priors:

$$-5 \leq \tilde{\rho}_s \equiv \log_{10}\left(\rho_s/[\text{GeV cm}^{-3}]\right) \leq 5\ ,$$
$$-5 \leq \tilde{r}_s \equiv \log_{10}\left(r_s/[\text{kpc}]\right) \leq 2$$
$$-3 \leq \tilde{r}_\beta \equiv \log_{10}\left(r_\beta/[\text{kpc}]\right) \leq 1$$
$$1 \leq b_0 \equiv 2^{\beta_0/(\beta_0-1)} \leq 1.95$$
$$0 \leq b_\infty \equiv 2^{\beta_\infty/(\beta_\infty-1)} \leq 1.95$$

gaussian priors:

$$\overline{D} \pm \Delta D$$
$$\overline{\alpha}_{1/2} \pm \Delta\alpha_{1/2}$$

matching observations

MCMC output of estimated parameters for Draco:

Petač, PU & Valli, 2018

Burkert:

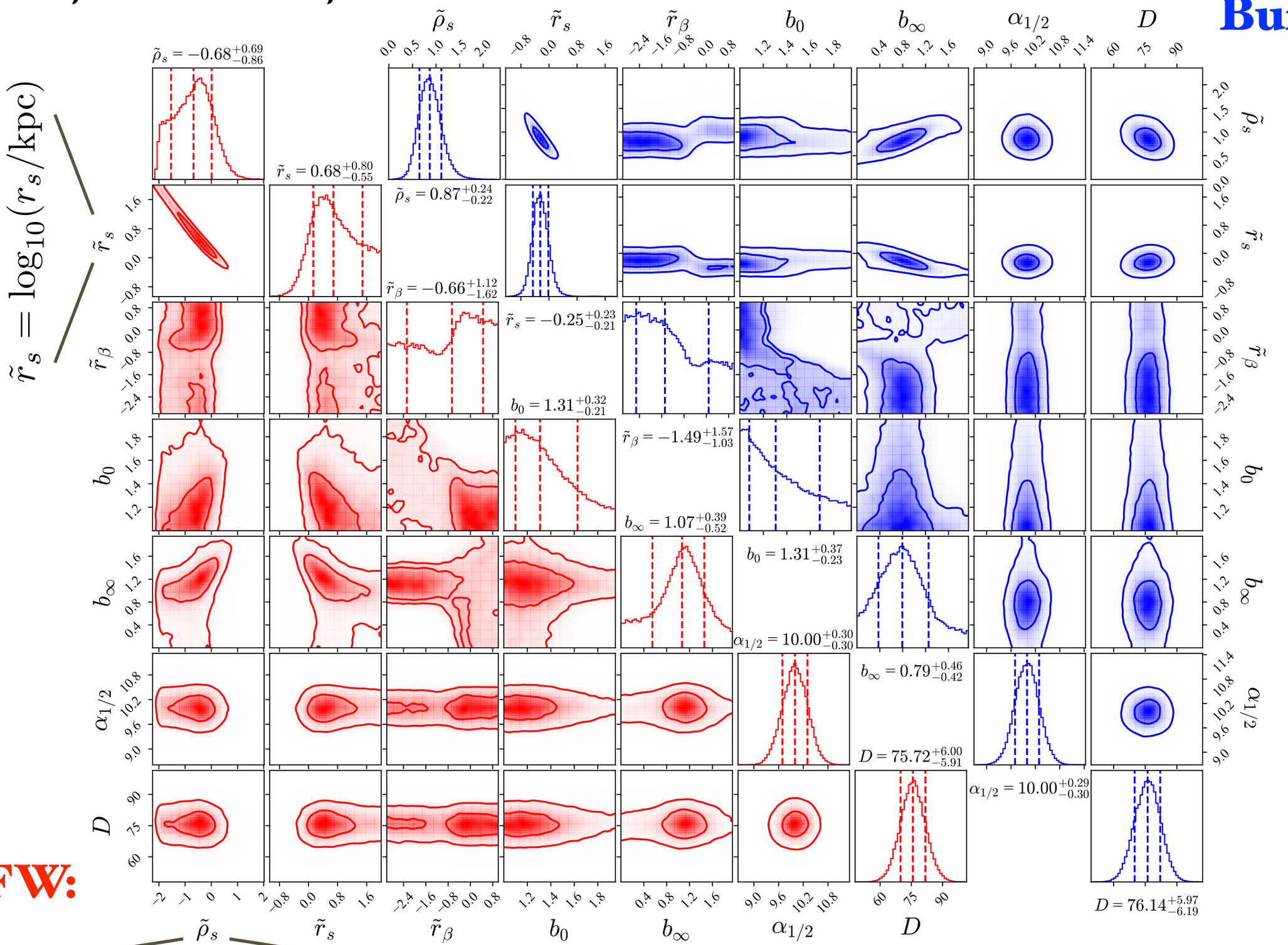

NFW:

$\tilde{\rho}_s = \log_{10}(\rho_s/\mathrm{GeV\,cm^{-3}})$

MCMC output of estimated parameters for Sculptor:

Petač, PU & Valli, 2018

Burkert:

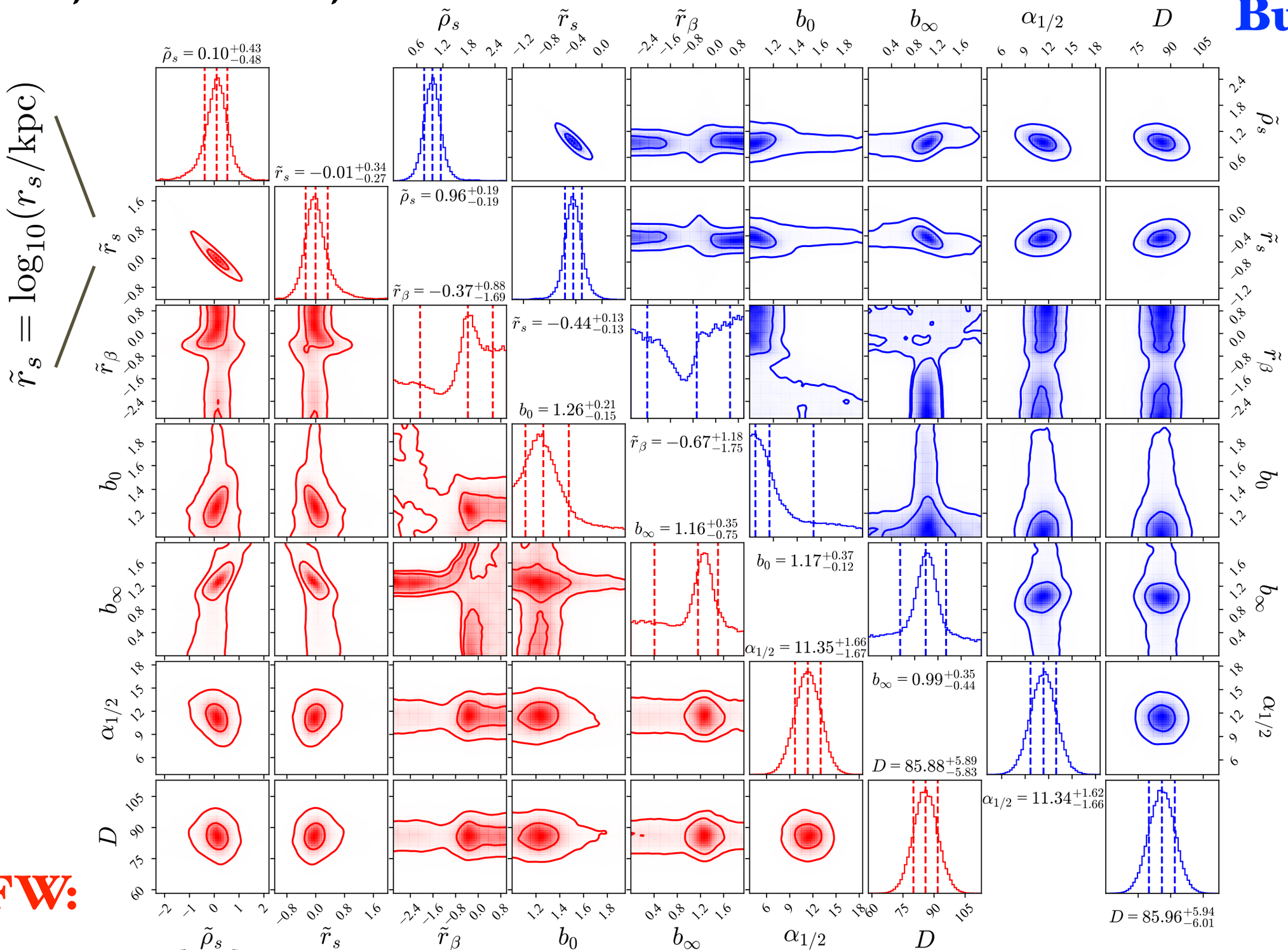

NFW:

$\tilde{r}_s = \log_{10}(r_s/\mathrm{kpc})$

$\tilde{\rho}_s = \log_{10}(\rho_s/\mathrm{GeV cm}^{-3})$

Posterior distributions for J-factors:

Output for the quantity relevant for WIMP (velocity independent) pair annihilations:

$$J \equiv \int_{\Delta\Omega} d\Omega \int_{\text{l.o.s.}} d\ell \, \rho^2(\vec{x})$$

NFW:

Burkert:

Draco:

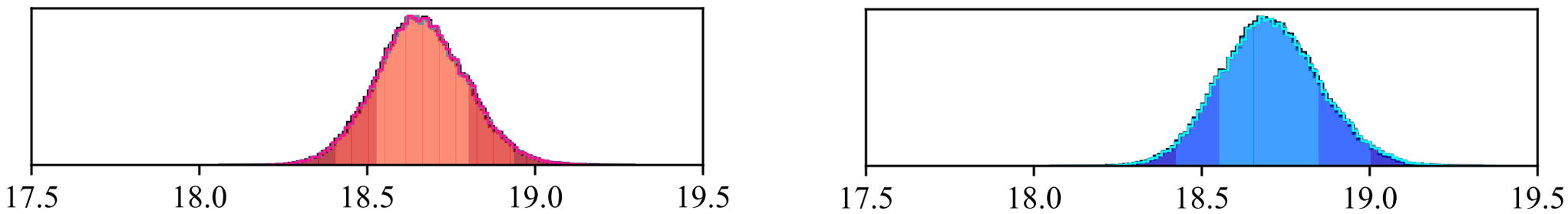

Sculptor:

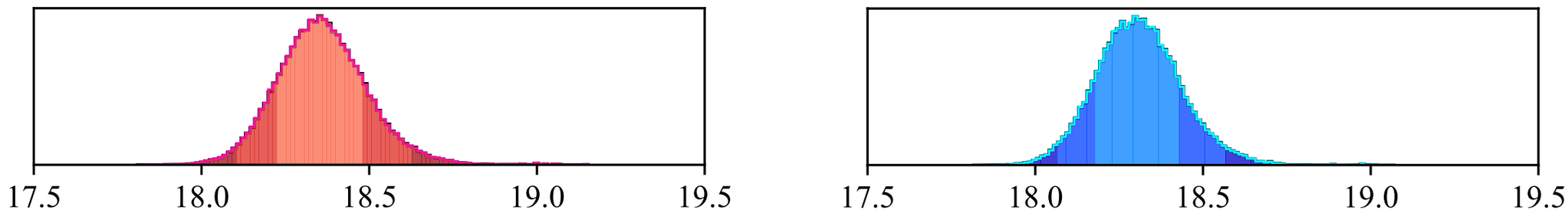

$\log_{10} J\,[\text{GeV}^2 / \text{cm}^5]$

$\log_{10} J\,[\text{GeV}^2 / \text{cm}^5]$

Petač, PU & Valli, 2018

Posterior distributions for J-factors (ii):

Output for the quantity relevant for WIMP (velocity independent) pair annihilations:

$$J \equiv \int_{\Delta\Omega} d\Omega \int_{\text{l.o.s.}} d\ell \, \rho^2(\vec{x})$$

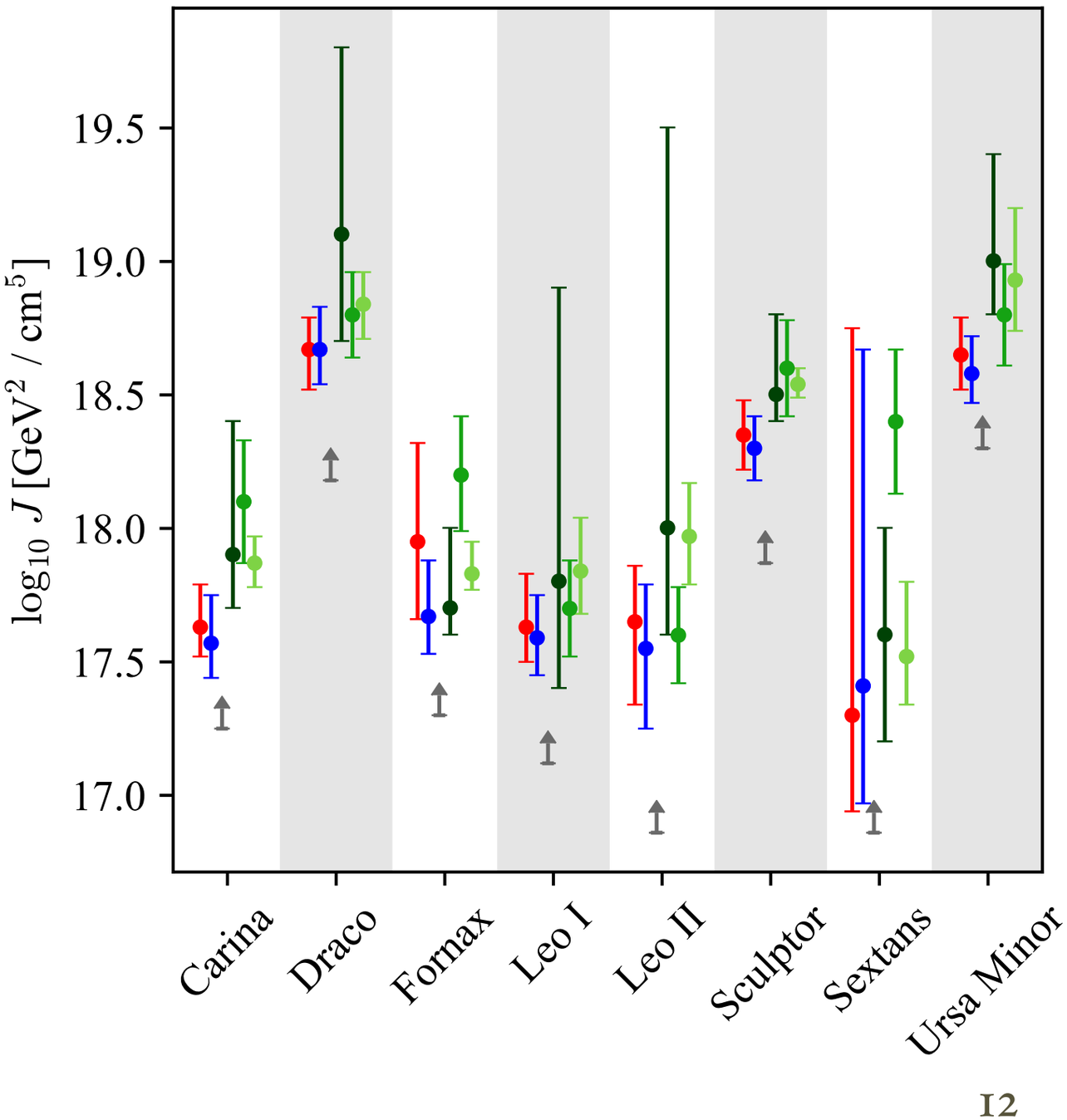

NFW
Burkert

Petač, PU & Valli, 2018

consistent with other recent previous (and specular) analyses, e.g.:

Bonnivard et al. 2015
Ackermann et al. 2014
Geringer-Sameth et al. 2015

Posterior distributions for J-factors (ii):

Output for the quantity relevant for WIMP (velocity independent) pair annihilations:

$$J \equiv \int_{\Delta\Omega} d\Omega \int_{\text{l.o.s.}} d\ell \, \rho^2(\vec{x})$$

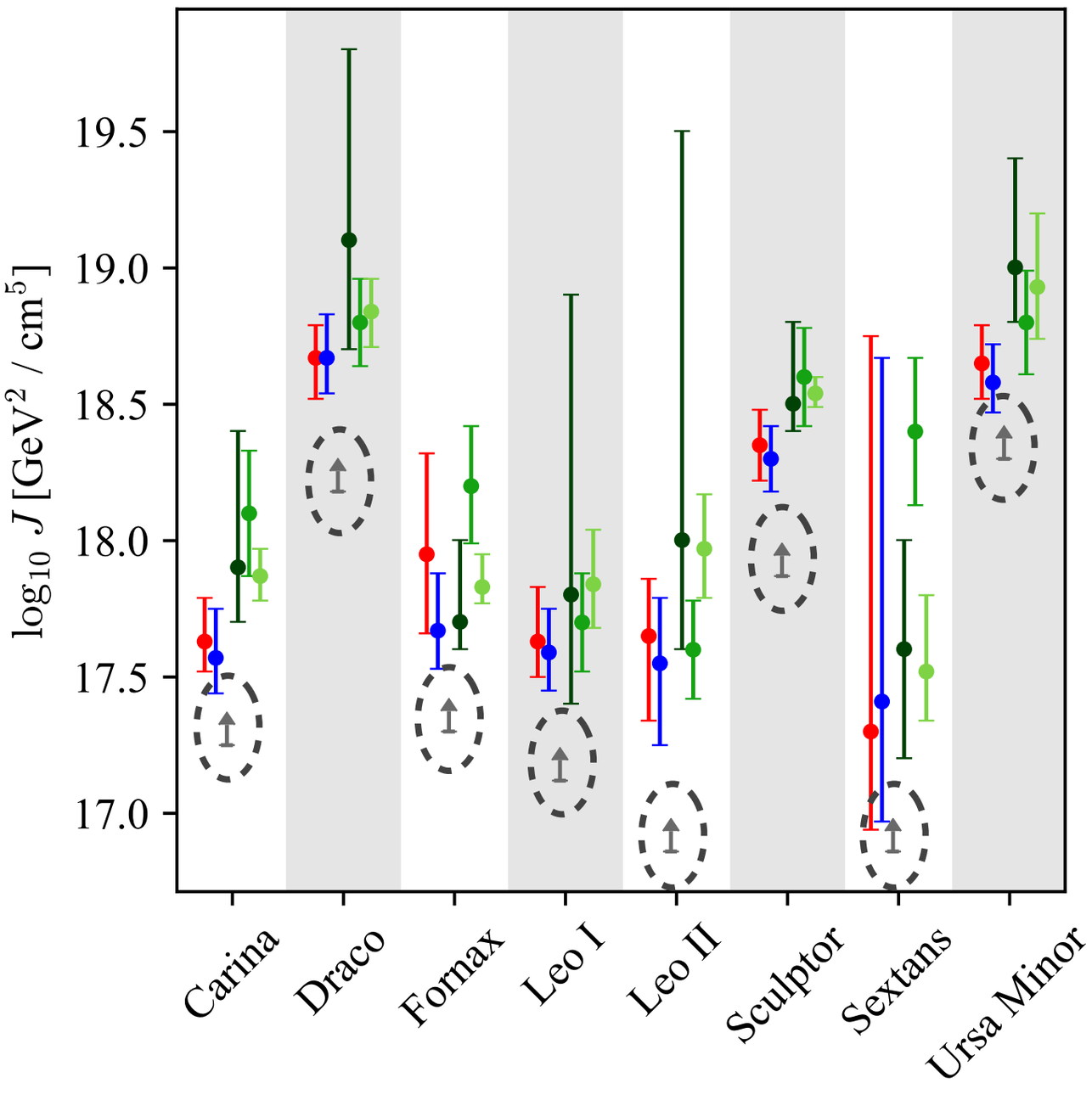

NFW
Burkert

Petač, PU & Valli, 2018

consistent with other recent previous (and specular) analyses, e.g.:

Bonnivard et al. 2015
Ackermann et al. 2014
Geringer-Sameth et al. 2015

One "pessimist" in the plot:

$\beta_\star \geq -\infty$

what is that???

An alternative mass model approach: (PU & Valli, 2016)

Stellar surface brightness: & the stellar l.o.s. velocity dispersion:

$$I_\star(R) = \int_R^\infty dr \frac{2r}{\sqrt{r^2 - R^2}} \nu_\star(r) \qquad \sigma^2_{los}(R) = \frac{1}{I_\star(R)} \int_R^\infty dr \frac{2r}{\sqrt{r^2 - R^2}} \left[1 - \beta_\star(r) \frac{R^2}{r^2}\right] p_\star(r)$$

are in a form which resembles an Abel integral transform for the pair $f \leftrightarrow \widehat{f}$

$$f(x) = \mathbf{A}[\widehat{f}(y)] = \int_x^\infty \frac{dy}{\sqrt{y - x}} \widehat{f}(y) \quad \longleftrightarrow \quad \widehat{f}(y) = \mathbf{A}^{-1}[f(x)] = -\frac{1}{\pi} \int_y^\infty \frac{dx}{\sqrt{x - y}} \frac{df}{dx}$$

Actually $I_\star(R^2) \leftrightarrow \widehat{I}_\star(r^2) = \nu_\star(r)$. Analogously you can invert also the projected dynamical pressure $P(R^2) \equiv I_\star(R)\, \sigma^2_{los}(R)$ and find:

$$M(r) = \frac{r^2}{G_N\, \widehat{I}(r)} \left\{ -\frac{d\widehat{P}}{dr}[1 - a_\beta(r)] + \frac{a_\beta(r)}{r} \cdot b_\beta(r) \left[\widehat{P}(r) + \int_r^\infty d\tilde{r} \frac{a_\beta(\tilde{r})}{\tilde{r}} \mathcal{H}_\beta(r, \tilde{r})\, \widehat{P}(\tilde{r}) \right] \right\}$$

having defined: $a_\beta(r) \equiv -\dfrac{\beta}{1 - \beta}$ $\qquad b_\beta(r) = 3 - a_\beta(r) - \dfrac{d \log a_\beta}{d \log r}$

$$\mathcal{H}_\beta(r, \tilde{r}) \equiv \exp\left(\int_r^{\tilde{r}} dr' \frac{a_\beta(r')}{r'} \right)$$

see also: **Wolf et al. 2010** + **Mamon & Boué 2009**.

An alternative mass model approach (ii):

Now: model $I_\star(R)$ and $\sigma_{los}(R)$ with a direct parametric fit on data for these observables. E.g.: assume for the surface brightness a Plummer model:

$$I_\star(R^2) = \frac{I_0}{\pi R_{1/2}^2} \frac{1}{(1 + R^2/R_{1/2}^2)^2}$$

and fit the half-light radius $R_{1/2}$ (i.e. in Ursa Minor: $R_{1/2} \simeq 0.3$ kpc).

For the line-of-sight projected velocity dispersion in general data are less constraining and one can consider different possibilities, e.g.:

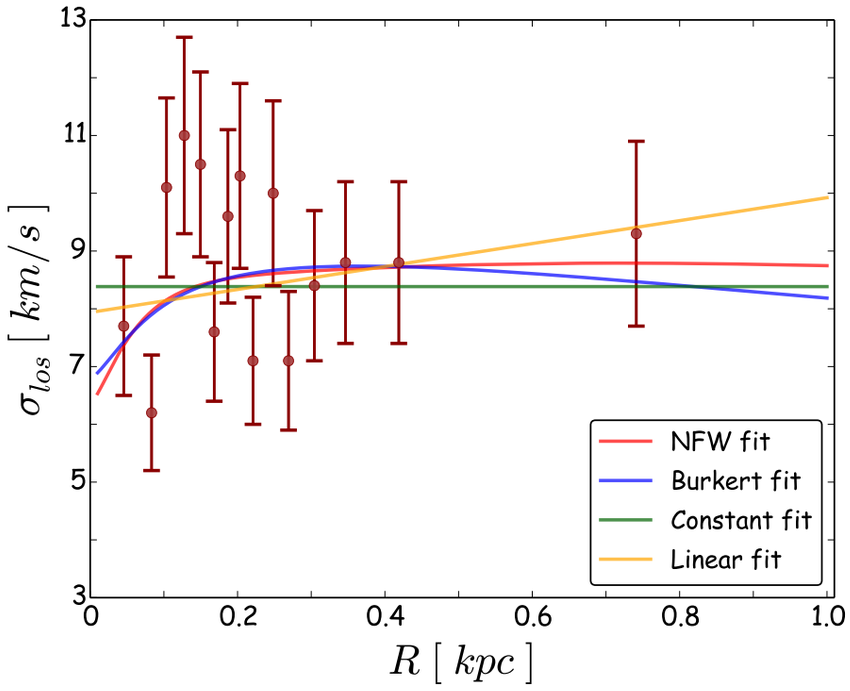

The Abel transforms $\widehat{P}(r)$ and $\widehat{I}_\star(r)$ are computed numerically, and then one can perform a direct projection of what you do (not) know about $\beta_\star(r)$ into a prediction for $M(r)$, $\rho(r)$ and J , and hence have a more direct assessment of uncertainties in the predictions for dark matter signals.

Mass profiles in Ursa Minor as a function of constant $\beta_\star$:

In practice, agnostic mass reconstruction with the inversion formula not always give physical results. In a concrete example we need to restrain (a posteriori) to cases in which we get $M(r) > 0$, $dM/dr > 0$ and $d\rho/dr \leq 0$:

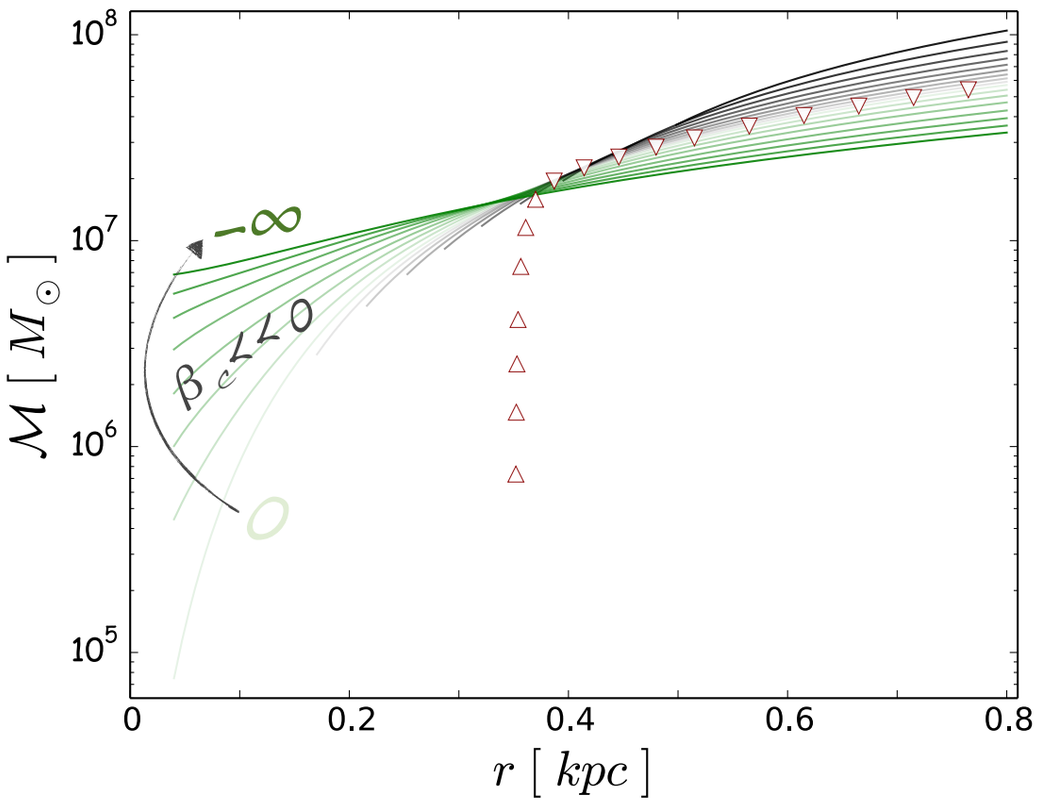

Burkert fit of the line-of-sight projected velocity dispersion: imposing radial orbits gives unphysical results at low radii

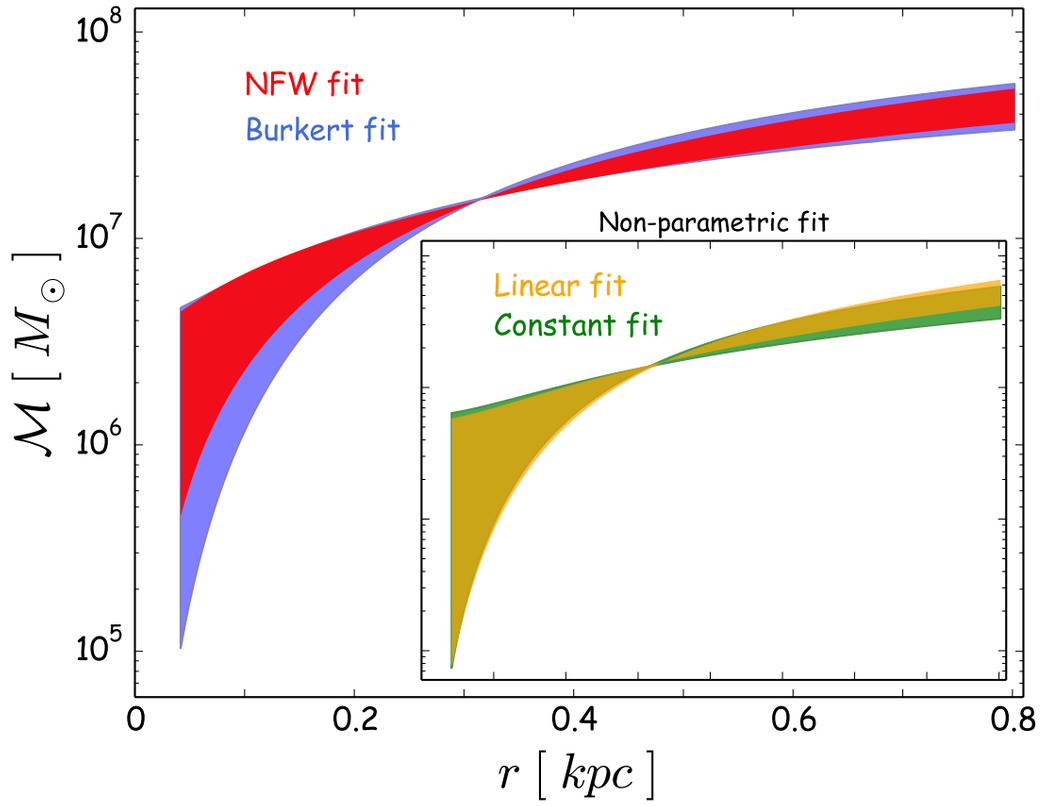

Span of results for 4 different possible fits of the line-of-sight projected velocity dispersion

Mass profiles in Ursa Minor as a function of constant $\beta_\star$:

In practice, agnostic mass reconstruction with the inversion formula not always give physical results. In a concrete example we need to restrain (a posteriori) to cases in which we get $M(r) > 0$, $dM/dr > 0$ and $d\rho/dr \leq 0$:

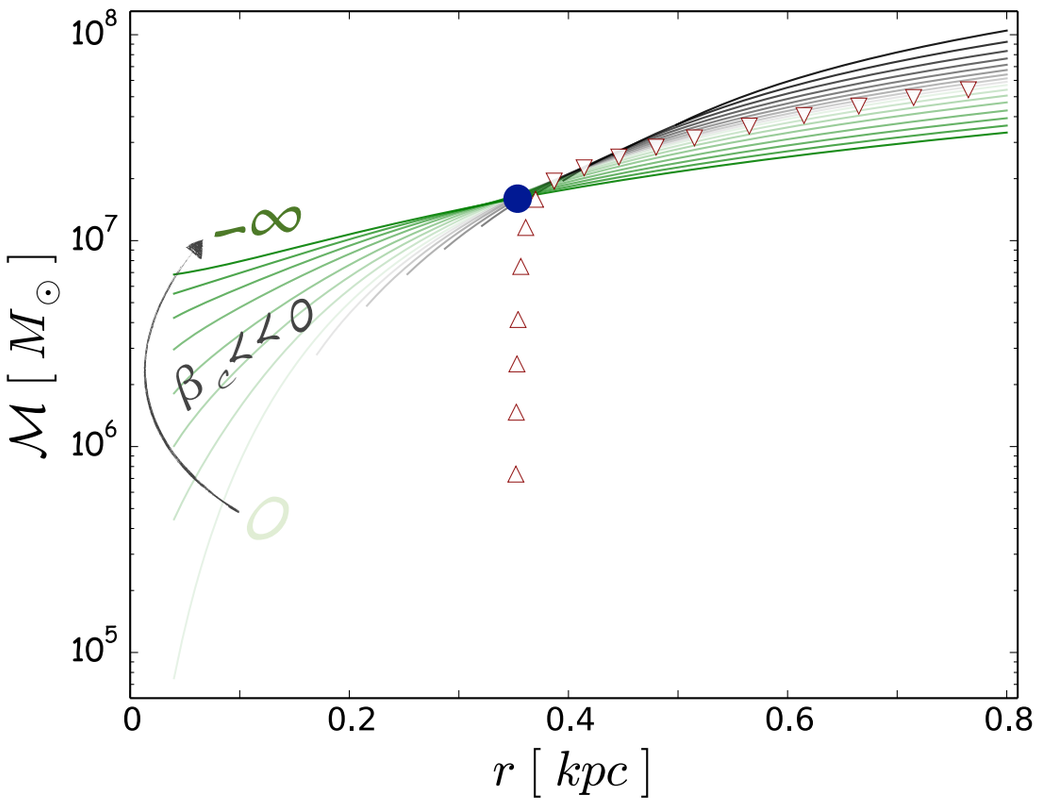

Burkert fit of the line-of-sight projected velocity dispersion: imposing radial orbits gives unphysical results at low radii

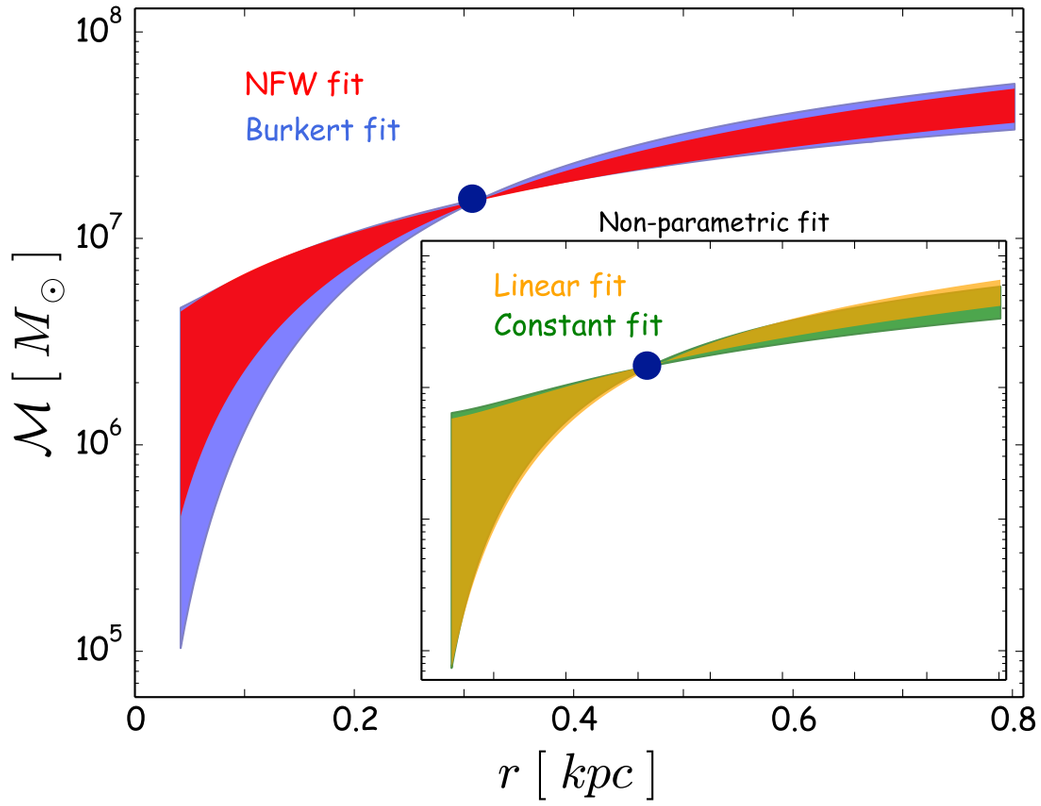

Span of results for 4 different possible fits of the line-of-sight projected velocity dispersion

Note: radius at which $M(r)$ is independent of $\beta_\star$!

Direct check on the existence of a mass estimator:

Claimed first from MCMC scans (**Strigari et al. 2008**) and then from the structure of the solution of Jeans' eq. (**Wolf et al. 2010**): after some algebra,

$$\mathcal{M}(r) - \mathcal{M}_{\beta_\star=0}(r) = -\frac{\beta_\star(r)\, r\, \sigma^2_{r,\star}}{G_N}\left(\frac{d\log \widehat{I}_\star}{d\log r} + \frac{d\log \sigma^2_{r,\star}}{d\log r} + \frac{d\log \beta_\star}{d\log r} + 3\right)$$

In case $\sigma_{r,\star}(r)$ and $\beta_\star(r)$ do not change rapidly with r , there is a radius r_* :

$$\left.\frac{d\log \widehat{I}_\star}{d\log r}\right|_{r=r_*} = -3 \quad \text{(i.e. } r_* = \sqrt{3/2}\, R_{1/2} \text{ for Plummer } I_\star\text{)} \longrightarrow \mathcal{M}(r_*) \simeq \mathcal{M}_{\beta=0}(r_*) \qquad \forall \quad \beta_\star$$

Check the mass differences compared to the isotropic case assuming constant $\beta_\star$ and σ_{los} :

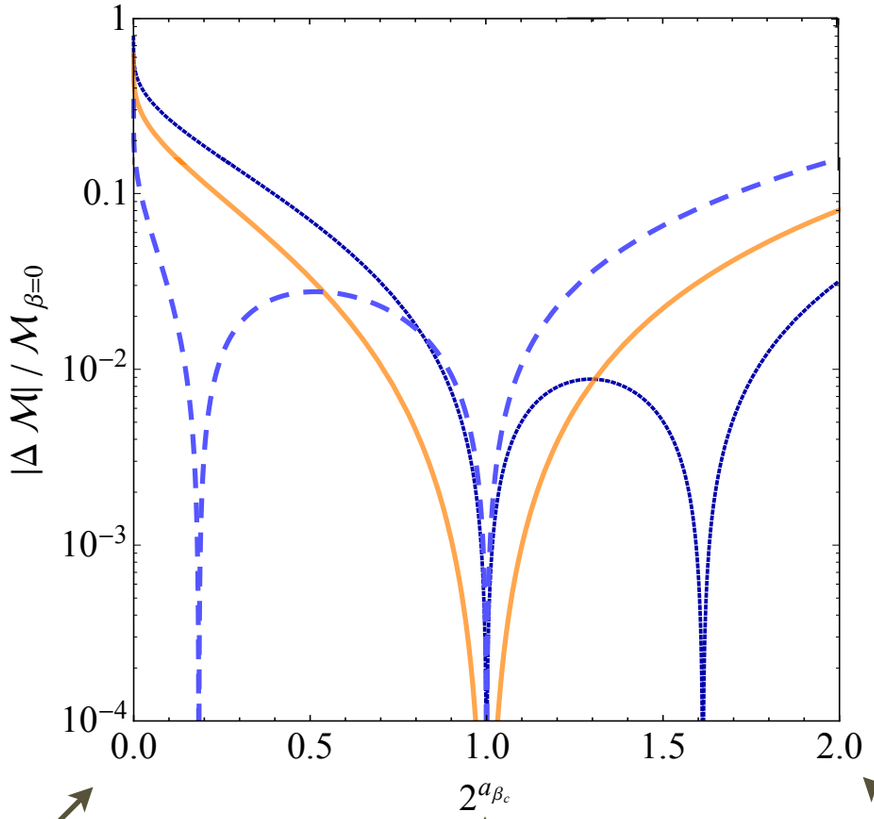

results at fixed radius:

- $r\,/\,r_* = 0.95$
- $r\,/\,r_* = 1.0$
- $r\,/\,r_* = 1.10$

Direct check on the existence of a mass estimator:

Claimed first from MCMC scans (**Strigari et al. 2008**) and then from the structure of the solution of Jeans' eq. (**Wolf et al. 2010**): after some algebra,

$$\mathcal{M}(r) - \mathcal{M}_{\beta_\star=0}(r) = -\frac{\beta_\star(r)\, r\, \sigma^2_{r,\star}}{G_N}\left(\frac{d\log \widehat{I}_\star}{d\log r} + \frac{d\log \sigma^2_{r,\star}}{d\log r} + \frac{d\log \beta_\star}{d\log r} + 3\right)$$

In case $\sigma_{r,\star}(r)$ and $\beta_\star(r)$ do not change rapidly with r , there is a radius r_* :

$$\left.\frac{d\log \widehat{I}_\star}{d\log r}\right|_{r=r_*} = -3 \quad \begin{array}{l}\text{(i.e. } r_* = \sqrt{3/2}\, R_{1/2} \\ \text{for Plummer } I_\star)\end{array} \longrightarrow \mathcal{M}(r_*) \simeq \mathcal{M}_{\beta=0}(r_*) \qquad \forall \quad \beta_\star$$

circular orbits →

isotropy →

radial orbits →

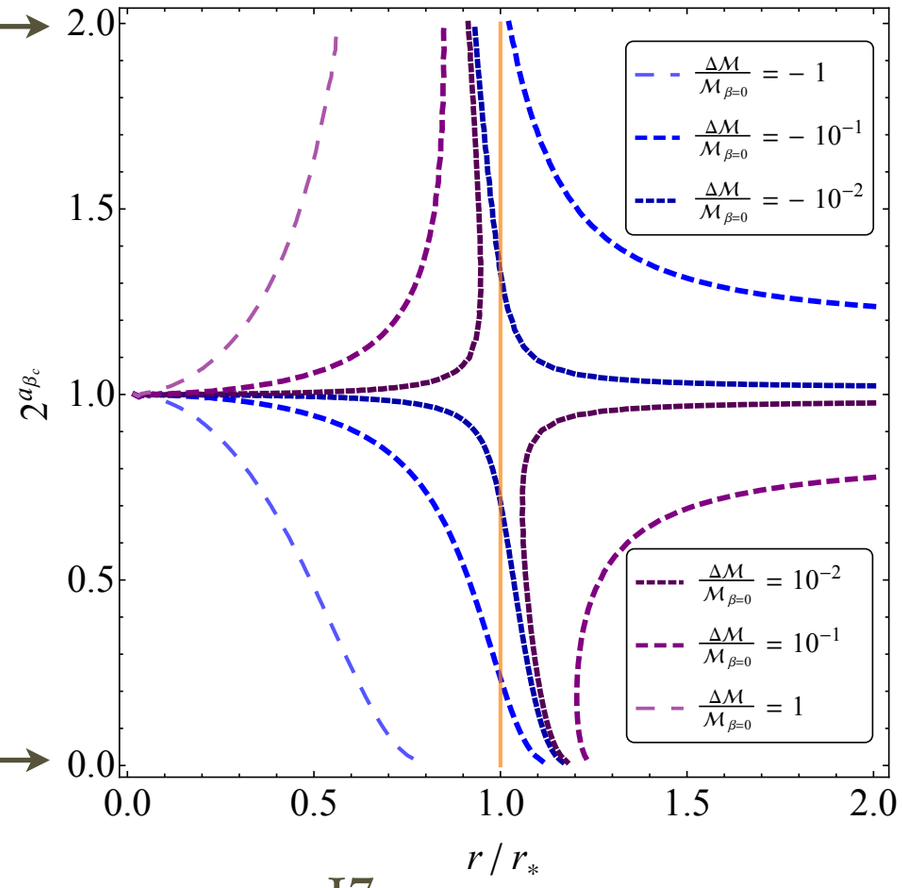

isolevel curves for the mass difference

Density profiles in Ursa Minor as a function of constant $\beta_\star$:

In practice, Density profiles are simply obtained from the first derivative of mass profiles; in analogy to the mass estimator, you can show that there is a density estimator (at a different radius r_{**}), as well as a logarithmic slope estimator, ect. ect. (**Petač, PU & Valli, 2018 to appear**)

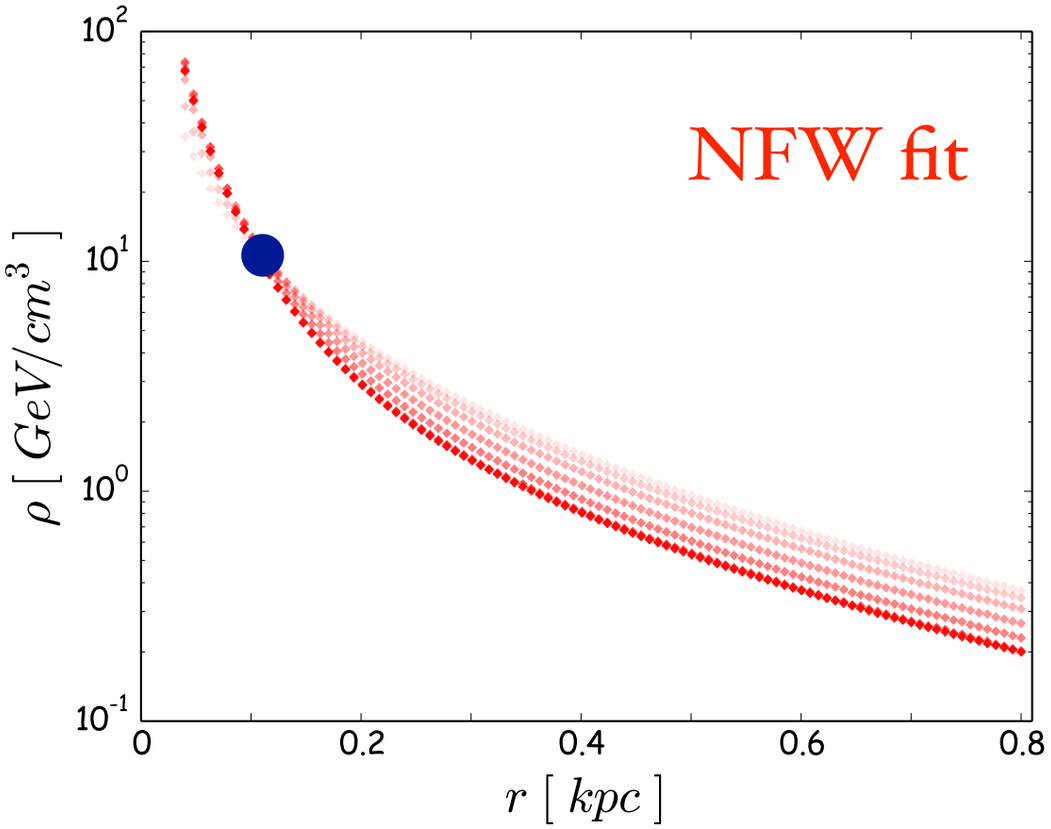

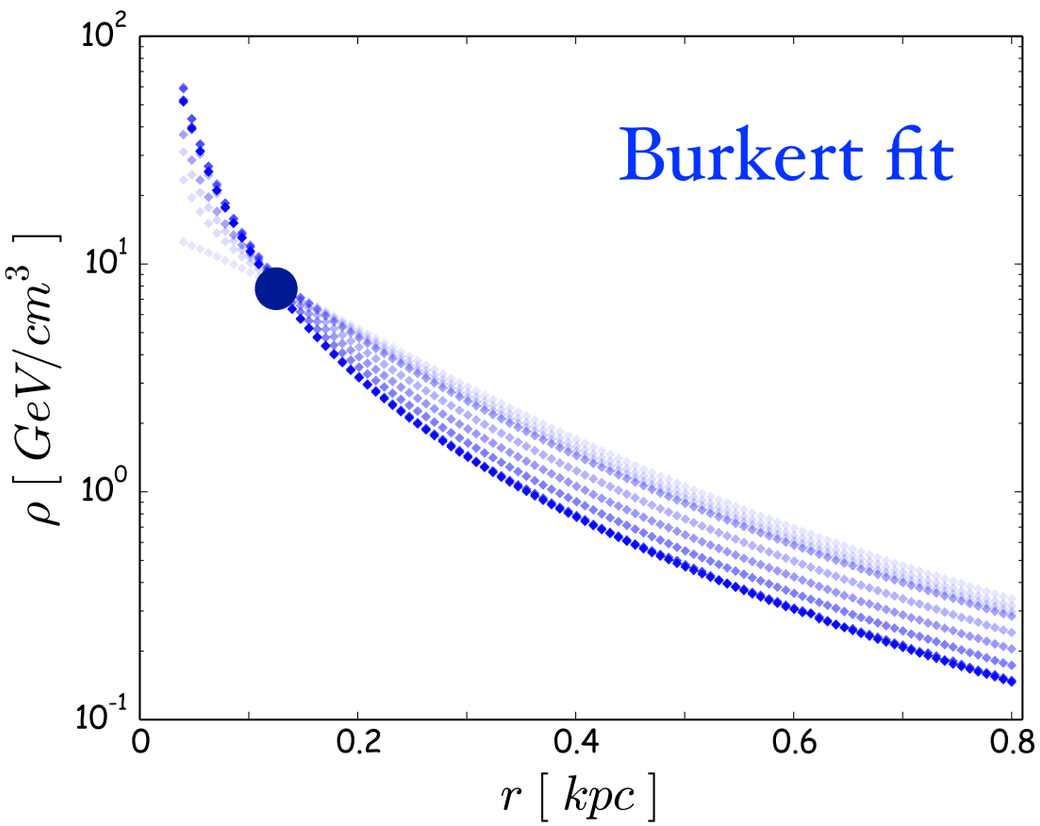

Sample behaviours at small radii:

- for $\sigma_{los}(R) = \text{const.}$, Plummer $I_\star$ + $\beta_\star = 0$ $\Rightarrow$ $\rho(r) \overset{r \to 0}{\simeq} \text{const}$
- for $\sigma_{los}(R) = \text{const.}$, Plummer $I_\star$ +$\beta_\star = -\infty$ $\Rightarrow$ $\rho(r) \overset{r \to 0}{\propto} r^{-1}$ + black hole

J-factors in Ursa Minor as a function of constant β:

In line-of-sight integrals: $J \equiv \int_{\Delta\Omega} d\Omega \int_{\mathrm{l.o.s.}} d\ell\, \rho^2(\vec{x})$

we conservative set $\rho(r)$ to a constant at radii smaller than the radius at which $\sigma_{l.o.s.}(R)$ can be measured (smallest radius in our data binning):

Span of predictions for the 4 sample fits of $\sigma_{l.o.s.}(R)$

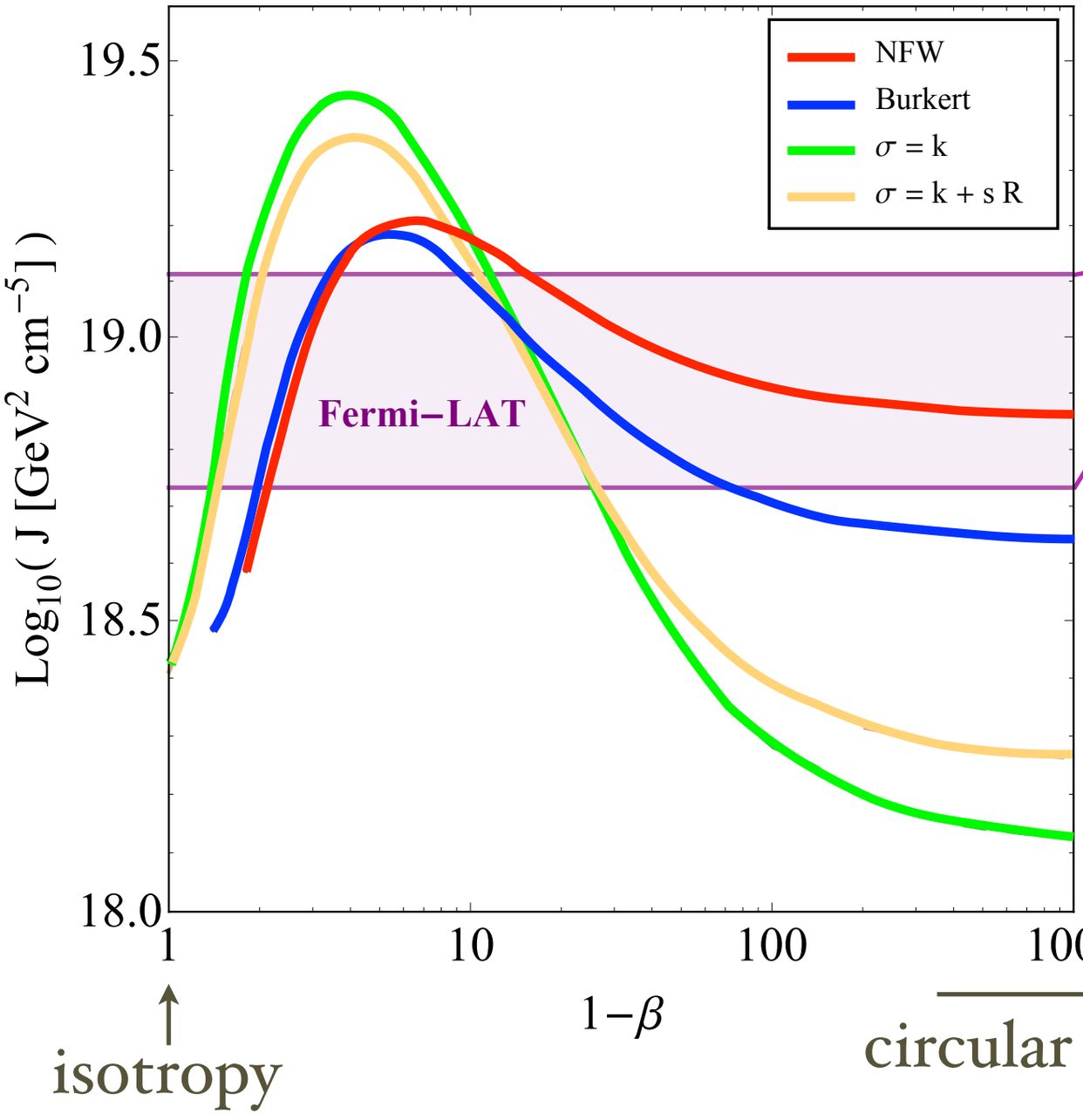

1-σ band for Ursa Minor in **Fermi Coll. 2015** apparently not fully catching the β uncertainty

J-factors in Ursa Minor as a function of constant β:

In line-of-sight integrals: $J \equiv \frac{1}{\Delta\Omega} \int_{\Delta\Omega} d\Omega \int_{l.o.s.} dl \; \rho^2_{DM}(l)$

we conservative set $\rho(r)$ to a constant at radii smaller than the radius at which $\sigma_{l.o.s.}(R)$ can be measured (smallest radius in our data binning):

Span of predictions for two possible parametric fits of $\sigma_{l.o.s.}(R)$

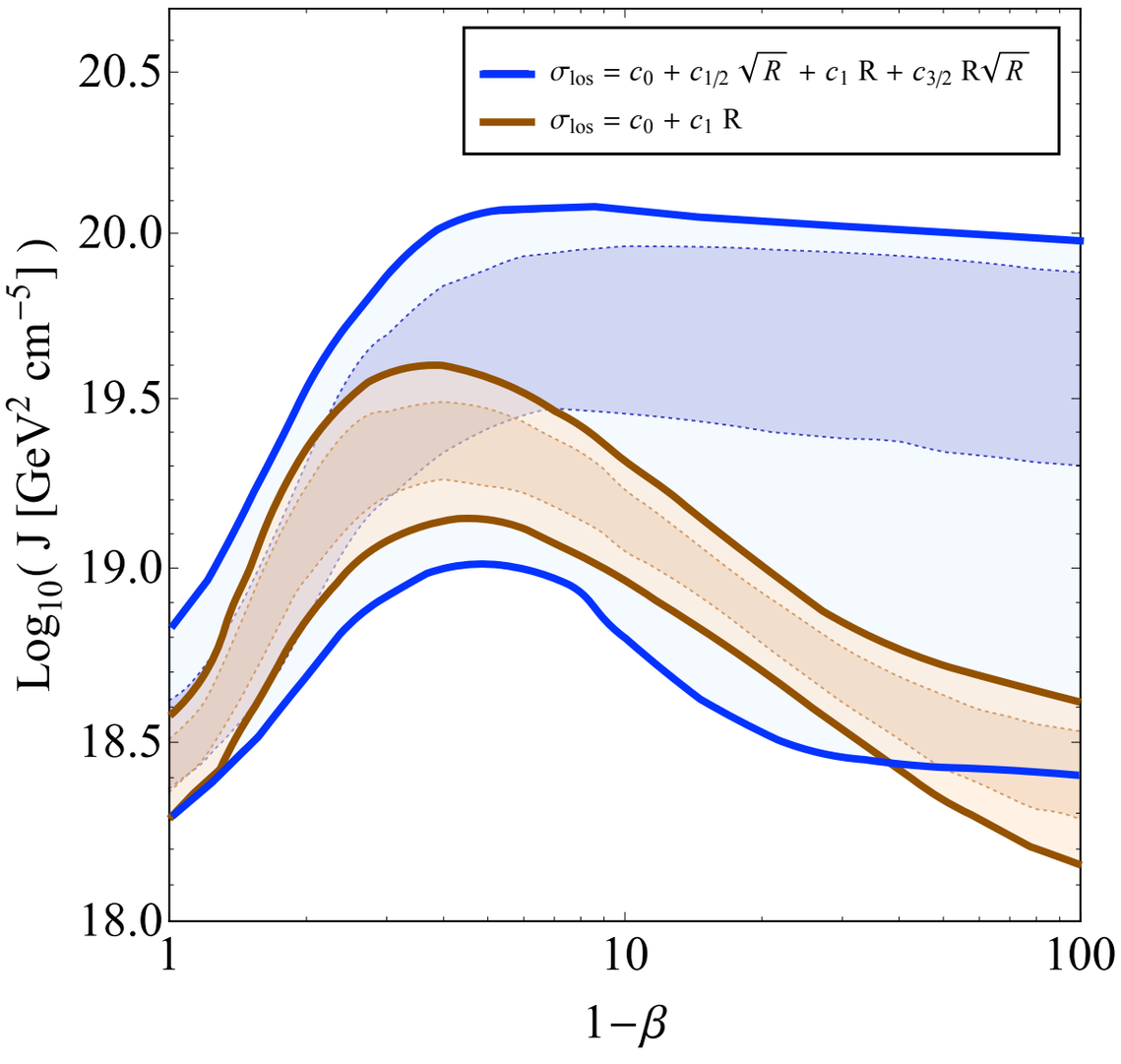

MCMC with flat priors on c_i coefficients; 68% and 95% contours for J posterior displayed

Take home message: current and projected limits from dwarfs need caution!

The case for velocity dependent WIMP annihilations

Suppose now that the DM pair annihilation cross section $(\sigma v_{\rm rel})$ has a non-trivial dependence on the modulus of the relative velocity $|\vec{v}_{\rm rel}| = |\vec{v}_1 - \vec{v}_2|$ of the two particles (1 & 2) in the pair. Introducing the factorisation:

$$(\sigma v_{\rm rel}) = (\overline{\sigma v}_{\rm rel}) \cdot S(|\vec{v}_{\rm rel}|)$$

and the DM phase-space distribution function (PSDF) $f_{\rm DM}(\vec{x}, \vec{v})$, the gamma-ray flux takes the form:

$$\frac{d\Phi_\gamma}{dE_\gamma} = \frac{1}{4\pi} \frac{(\overline{\sigma v}_{\rm rel})}{2m_\chi^2} \frac{dN_\gamma}{dE_\gamma} \int_{\Delta\Omega} d\Omega \int_{\rm l.o.s.} d\ell \int d\vec{v}_1 f_{\rm DM}(\vec{x}, \vec{v}_1) \int d\vec{v}_2 \; f_{\rm DM}(\vec{x}, \vec{v}_2) \, S(|\vec{v}_{\rm rel}|)$$

$$\equiv \int_{\Delta\Omega} d\Omega \int_{\rm l.o.s.} d\ell \, \rho^2{}_{\rm DM}(\vec{x}) \; \langle S(v_{\rm rel}) \rangle (\vec{x}) \equiv J$$

generalisation of the J-factor

If $S(|\vec{v}_{\rm rel}|)$ gives an enhancement in the low $|\vec{v}_{\rm rel}|$ limit, such as in case of Sommerfeld enhancement, dwarfs are again an ideal target, since they are small objects with fairly low DM velocity dispersions.

In this case, critical to infer from observations $f_{\rm DM}(\vec{x}, \vec{v})$ rather than $\rho(r)$

PSDF under different approximations/assumptions:

Early analyses have considered a Maxwell-Boltzmann velocity distribution with constant velocity dispersion (isothermal sphere model); in general this approximation is too crude.

A first readjustment by considering the spherical Jeans equation (now applied to DM rather than stars), in the isotropic limit ($\beta_{\rm DM} = 0$) to find a radially dependent velocity dispersion:

$$\sigma^2_{\rm DM}(r) = \frac{1}{\rho_{\rm DM}(r)} \int_r^\infty dr' \rho_{\rm DM}(r') \frac{d\Phi}{dr'}$$

The approximate ***Maxwell-Boltzmann*** type PSDF takes the form:

$$f_{\text{DM-MB}}(r, v) = \frac{\rho_{\rm DM}(r)}{(2\pi\sigma^2_{\rm DM}(r))^{3/2}} \cdot \exp\left[-v^2 / \left(2\sigma^2_{\rm DM}(r)\right)\right]$$

This form is particularly handy since all velocity integrals in $\langle S(v_{\rm rel})\rangle$, except for the one on $|\vec{v}_{\rm rel}|$, can be performed analytically.

PSDF under different approximations/assumptions (ii):

Spherical isotropic systems have a PSDF depending only on the particle energy. Expressing this dependence in terms of the relative energy:

$$\mathcal{E} \equiv \Psi(r) - \frac{v^2}{2}$$

being the relative potential $\Psi(r) \equiv \Phi_b - \Phi(r)$ a monotonic function, you can treat $\rho_{\rm DM}$ as a function of Ψ and invert the expression:

$$\rho_{\rm DM}(r) = \int d^3v \; f_{\rm DM}(r, v)$$

to find the so-called ***Eddington's inversion formula***:

$$f_{\text{DM-E}}(\mathcal{E}) = \frac{1}{\sqrt{8}\pi^2} \frac{d}{d\mathcal{E}} \int_0^{\mathcal{E}} \frac{d\Psi}{\sqrt{\mathcal{E} - \Psi}} \frac{d\rho_{\rm DM}}{d\Psi}$$

This formula can be applied to compute numerically the ergodic PSDF for any spherical density profile; the 6-dimensional integral in $\langle S(v_{\rm rel}) \rangle$ can be reduced to a 3-dimensional integral.

PSDF under different approximations/assumptions (iii):

More generically, the PSDF of a non-isotropic spherical system, besides $\mathcal{E}$, depends also on the magnitude of the angular momentum L. Such distributions can be radially biased or tangentially biased, depending on the sign of the DM anisotropy parameter $\beta_{\rm DM}$. Sample setups for both cases:

1) The ***Osipkov-Meritt*** model with increasing radial bias in the outskirts:

$$\beta_{\rm DM}(r) = \frac{r^2}{r^2 + r_a^2}$$

in this case the PSDF still depends on a single quantity, $Q \equiv \mathcal{E} - L^2/(2r_a^2)$, and there is an inversion formula specular to Eddington's formula:

$$f_{\text{DM-OM}}(Q) = \frac{1}{\sqrt{8}\pi^2}\frac{d}{dQ}\int_0^Q \frac{d\Psi}{\sqrt{Q-\Psi}}\frac{d\rho_{\text{DM-Q}}}{d\Psi}$$

2) In models with ***constant negative*** $\beta_{\rm DM}$, the PSDF can be factorised:

$$f_{\text{DM}-\beta_c}(\mathcal{E}, L) = \left(\frac{L}{L_0}\right)^{-2\beta_c} \cdot g_{\beta_c}(\mathcal{E}, L_0)$$

For any half-integer β_c, the inversion is again similar Eddington's formula and is particularly simple for:

$$\beta_c = -1/2 \qquad \longrightarrow \qquad g_{-1/2}(\Psi, L_0) = \frac{L_0}{2\pi^2}\frac{\mathrm{d}^2}{\mathrm{d}\Psi^2}\left(\frac{\rho_{\rm DM}}{r}\right)$$

Velocity probability distributions for the 4 models:

The 4 PSDF introduced above are constructed from the same density profile $\rho(r)$, as constrained from the same gravitational potential well Ψ.

Nevertheless, they introduce a significant degree of uncertainty when computing J-factors for velocity dependent WIMP annihilations. Get a feeling of the differences at the level of 1-particle velocity probability distributions:

$$\mathrm{P}(v;r) = \frac{v^2}{\rho_{\mathrm{DM}}(r)} \int d\Omega_v f_{\mathrm{DM}}(r,\vec{v})$$ (integral over velocity direction)

NFW:

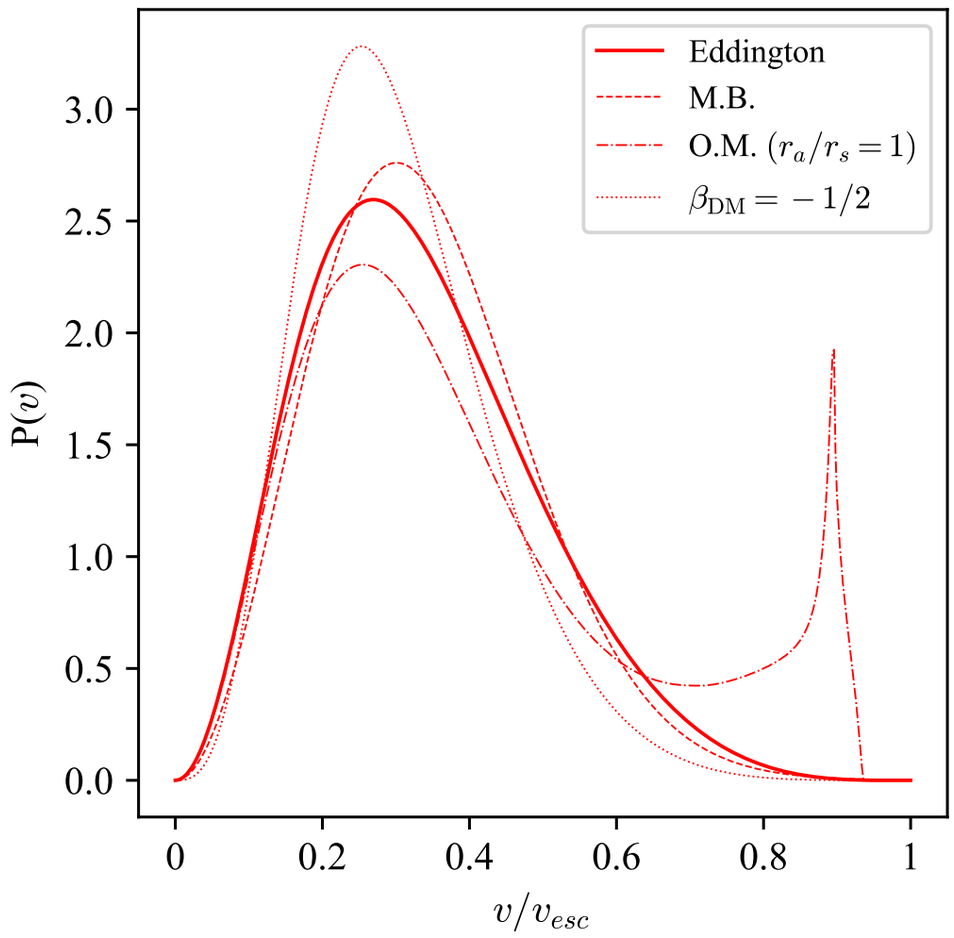

Burkert:

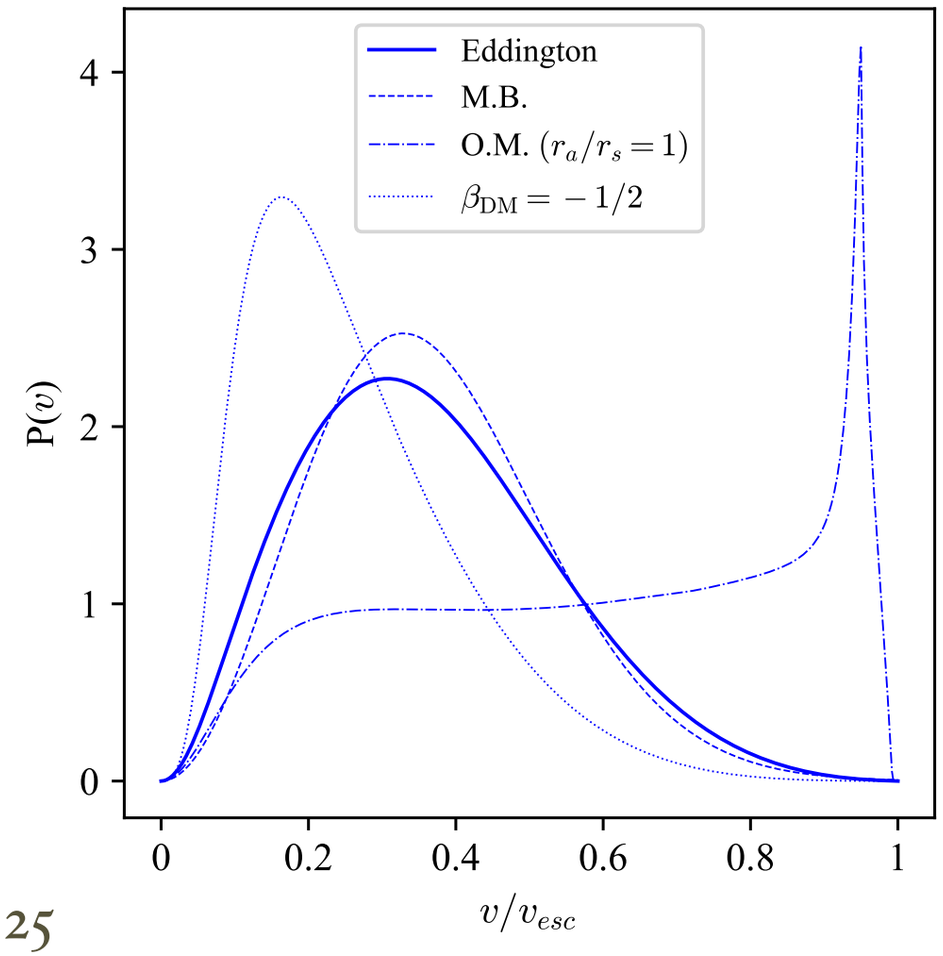

Prototype for the velocity dependent WIMP annihilation case:

Sommerfeld effect: the strong enhancement in $(\sigma v_{\rm rel})$ for highly non-relativistic (slow) particles subject to a long-range force. E.g.: DM particles χ annihilating through the light mediator ϕ $(m_\chi \gg m_\phi)$; in this case the velocity dependent pre-factor is approximately:

$$S(v_{\rm rel};\,\xi) \simeq \frac{\pi\alpha_\chi}{v_{\rm rel}} \frac{\sinh\left(\frac{12 v_{\rm rel}}{\pi\alpha_\chi \xi}\right)}{\cosh\left(\frac{12 v_{\rm rel}}{\pi\alpha_\chi \xi}\right) - \cos\left(2\pi\sqrt{\frac{6}{\pi^2\xi} - \left(\frac{6 v_{\rm rel}}{\pi^2\alpha_\chi\xi}\right)^2}\right)}$$

with $\xi \equiv m_\phi / (\alpha_\chi m_\chi)$ and α_χ the long-range coupling constant.

Three distinct regimes:

i) large $v_{\rm rel}$ or $m_\phi \gtrsim m_\chi$: $\quad S(v_{\rm rel};\,\xi \gg 1) \to 1$

ii) vanishing mediator mass (Coulomb regime): $\quad S(v_{\rm rel};\,\xi \ll 1) \approx \frac{\pi\alpha_\chi}{v_{\rm rel}}$

iii) resonant regime: $\quad S(v_{rel}\,;\,\xi_{\rm res} = \frac{6}{\pi^2 n^2}) \approx \frac{\alpha_\chi^2}{v_{\rm rel}^2 n^2}$ $\quad$ for each $\quad n \in \mathbb{N}$

J-factor estimates from PSDFs:

While for a single parametric model the computation of the J-factor is numerically demanding (numerical computation of the PSDF; 3 integrals to compute $\langle S(v_{\rm rel})\rangle(r)$ at any radius r + its folding into the l.o.s.i. for J) one can make it modular and apply scaling relations, so that the computation of posterior distributions on a full MCMC chain becomes viable:

Draco:

Petač, PU & Valli, 2018

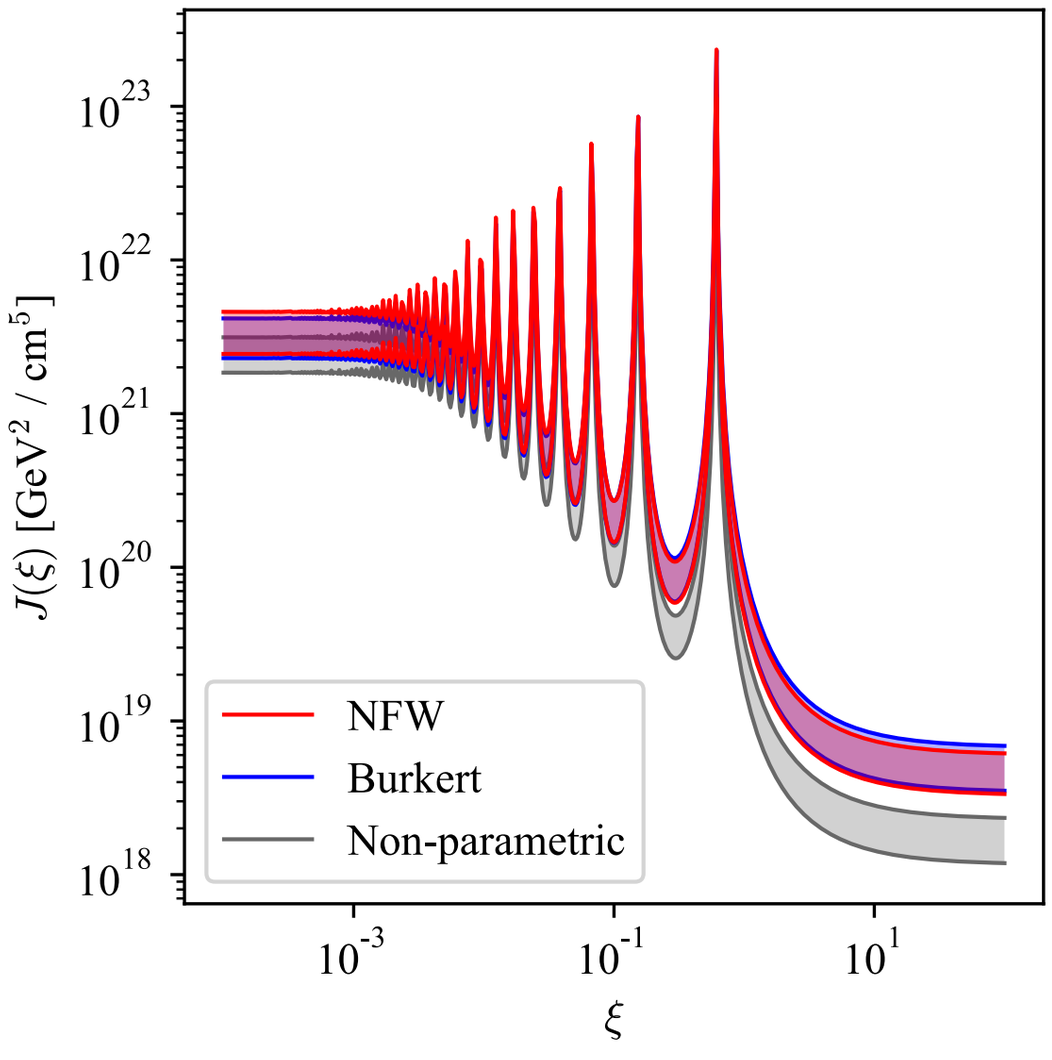

$$J = \int_{\Delta\Omega} d\Omega \int_{\rm l.o.s.} d\ell\, \rho^2{}_{\rm DM}(\vec{x})\ \langle S(v_{\rm rel})\rangle(\vec{x})$$

68% highest density probability regions from the MCMC discussed above, assuming a PSDF according to the Eddington isotropic model

J-factor estimates from PSDFs:

While for a single parametric model the computation of the J-factor is numerically demanding (numerical computation of the PSDF; 3 integrals to compute $\langle S(v_{\rm rel})\rangle(r)$ at any radius r + its folding into the l.o.s.i. for J) one can make it modular and apply scaling relations, so that the computation of posterior distributions on a full MCMC chain becomes viable:

Sculptor:

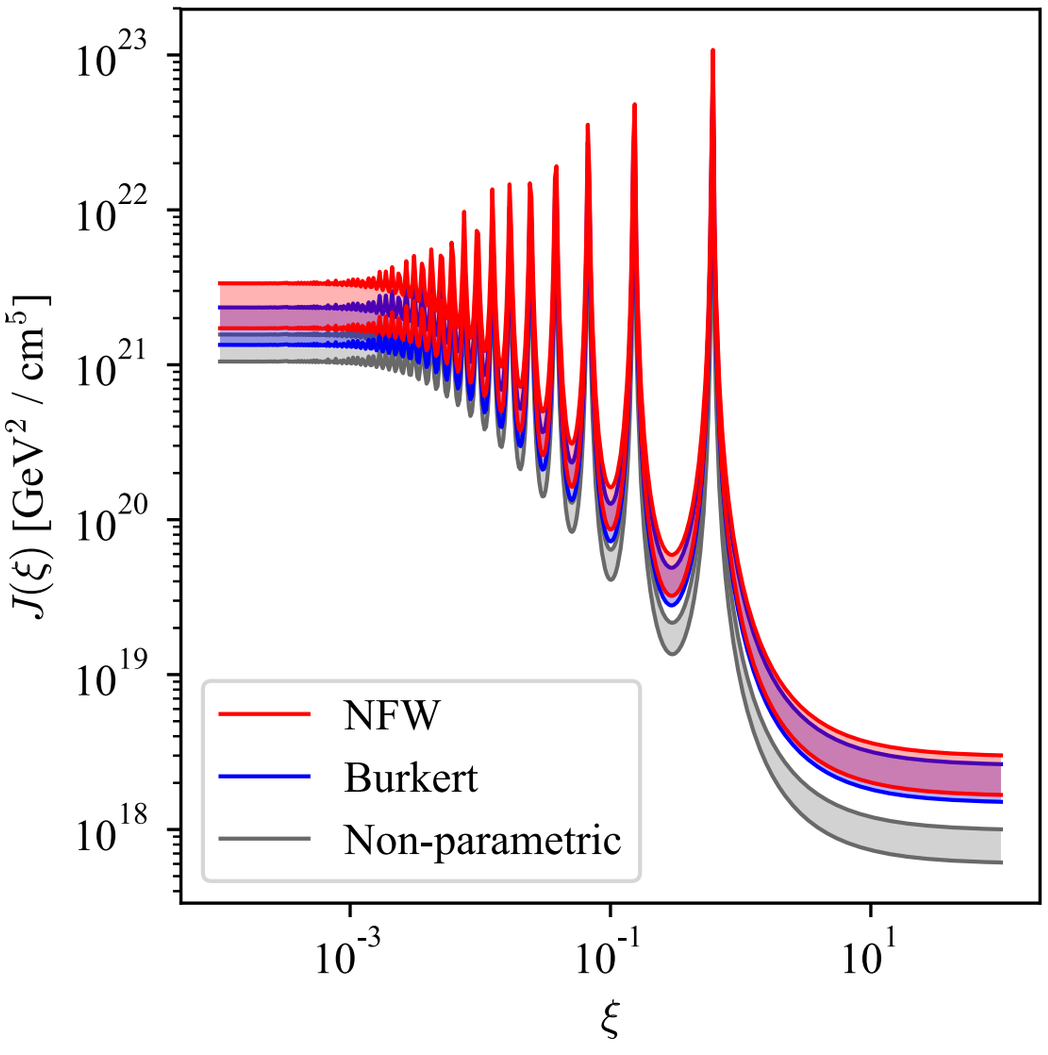

Petač, PU & Valli, 2018

$$J = \int_{\Delta\Omega} d\Omega \int_{\rm l.o.s.} d\ell\, \rho^2{}_{\rm DM}(\vec{x})\ \langle S(v_{\rm rel})\rangle(\vec{x})$$

68% highest density probability regions from the MCMC discussed above, assuming a PSDF according to the Eddington isotropic model

J-factor estimates from PSDFs:

Results for the 4 PSDF introduced above:

Draco:

NFW:

Burkert:

Coulomb regime

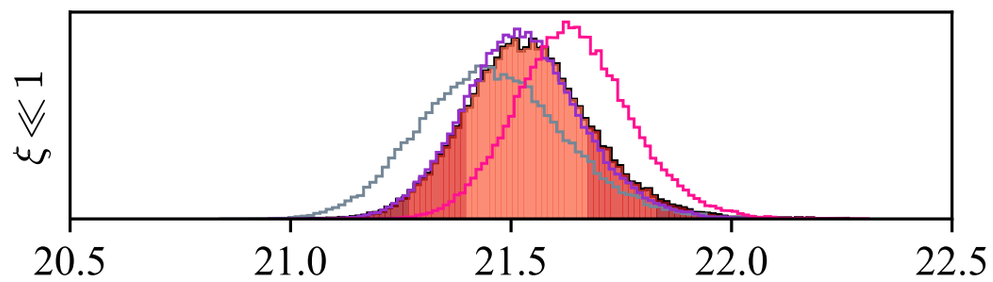

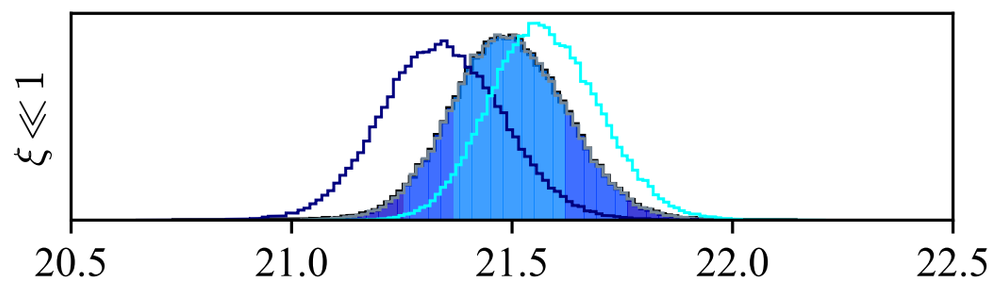

resonant regime

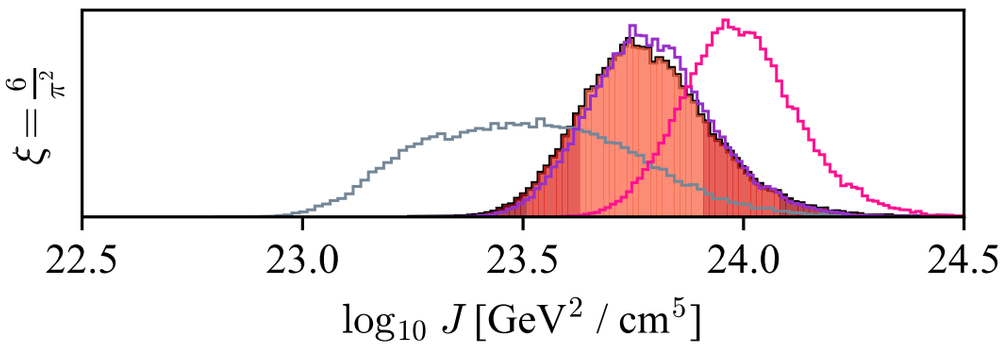

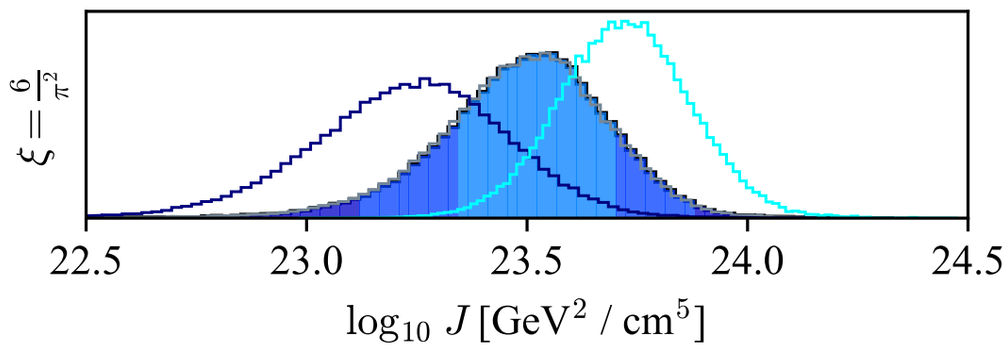

Petač, PU & Valli, 2018

J-factor estimates from PSDFs:

Results for the 4 PSDF introduced above:

Draco:

NFW:

Burkert:

Coulomb regime

resonant regime

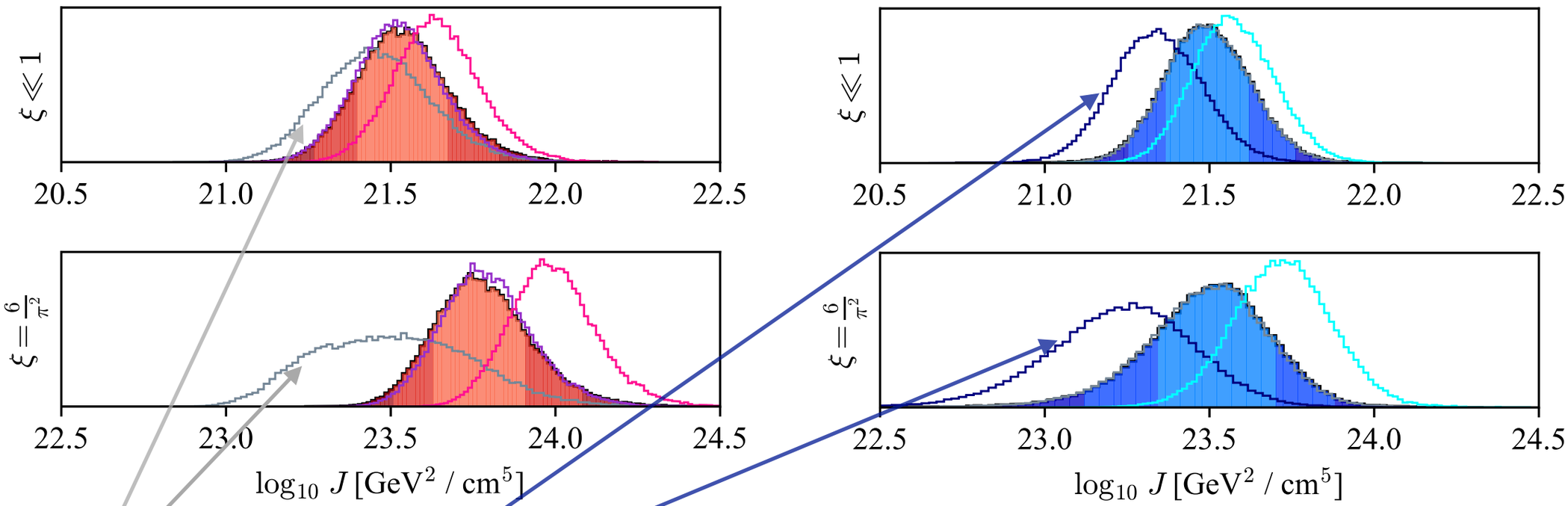

Maxwell-Boltzmann

Petač, PU & Valli, 2018

J-factor estimates from PSDFs:

Results for the 4 PSDF introduced above:

Draco:

NFW:

Burkert:

Coulomb regime

resonant regime

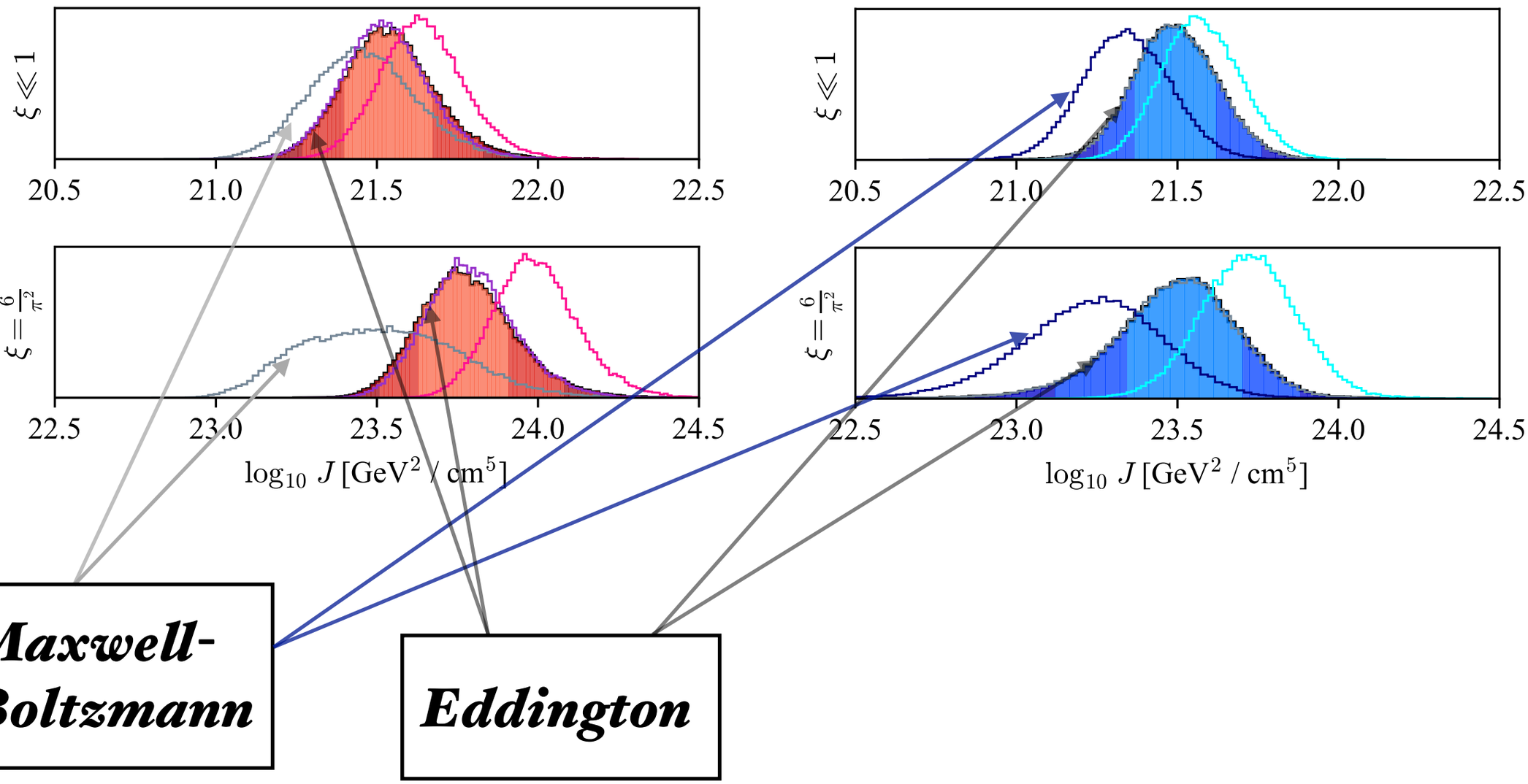

Maxwell-Boltzmann

Eddington

Petač, PU & Valli, 2018

J-factor estimates from PSDFs:

Results for the 4 PSDF introduced above:

Draco:

NFW:

Burkert:

Coulomb regime

resonant regime

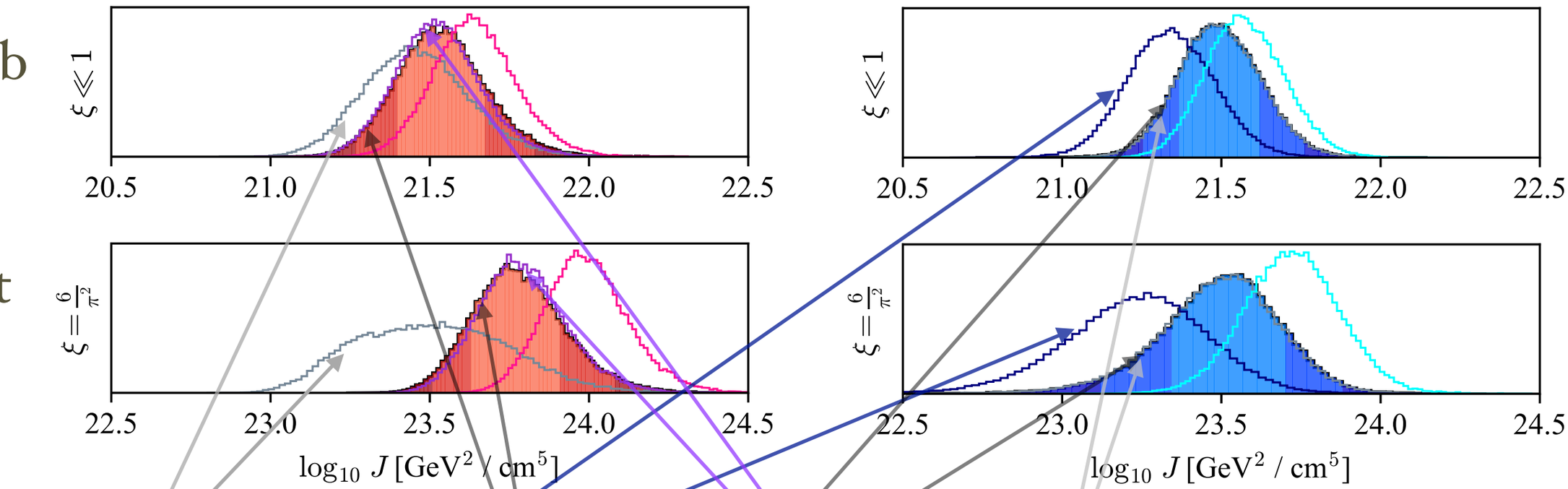

Maxwell-Boltzmann

Eddington

Osipkov-Meritt

Petač, PU & Valli, 2018

J-factor estimates from PSDFs:

Results for the 4 PSDF introduced above:

Draco:

NFW:

Burkert:

Coulomb regime

resonant regime

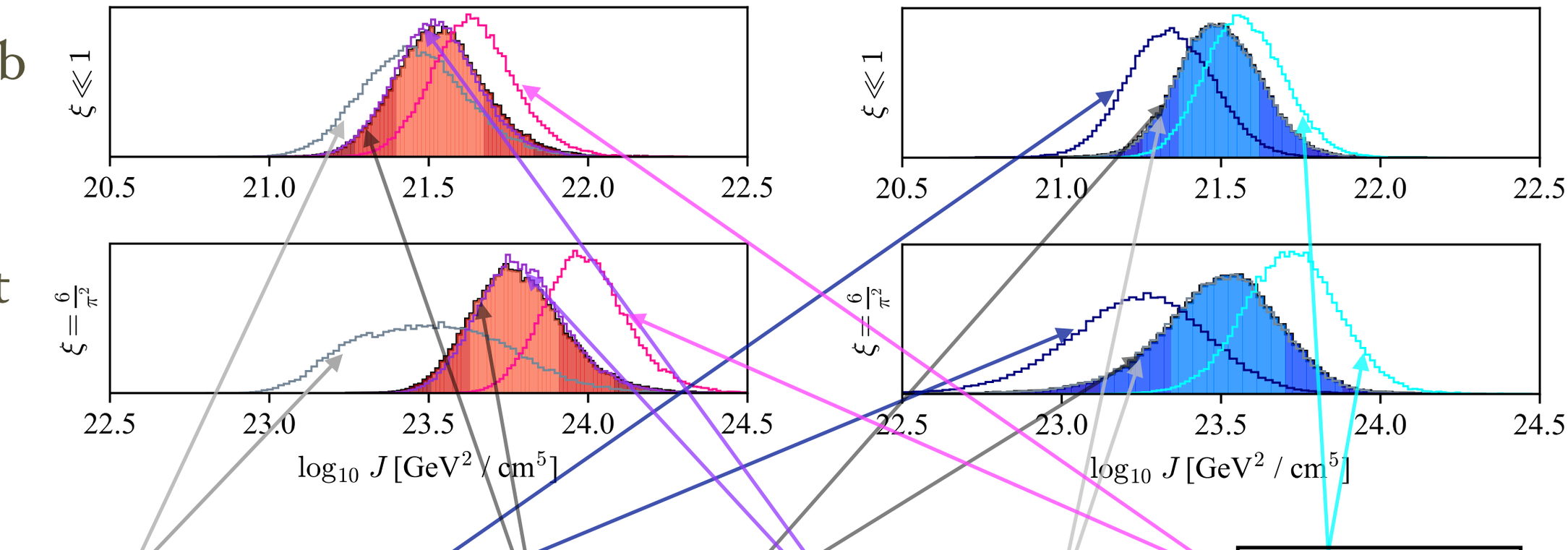

Maxwell-Boltzmann

Eddington

Osipkov-Meritt

$\beta_c = -1/2$

Petač, PU & Valli, 2018

J-factor estimates from PSDFs:

Results for the 4 PSDF introduced above:

Sculptor:

NFW:

Burkert:

Coulomb regime

resonant regime

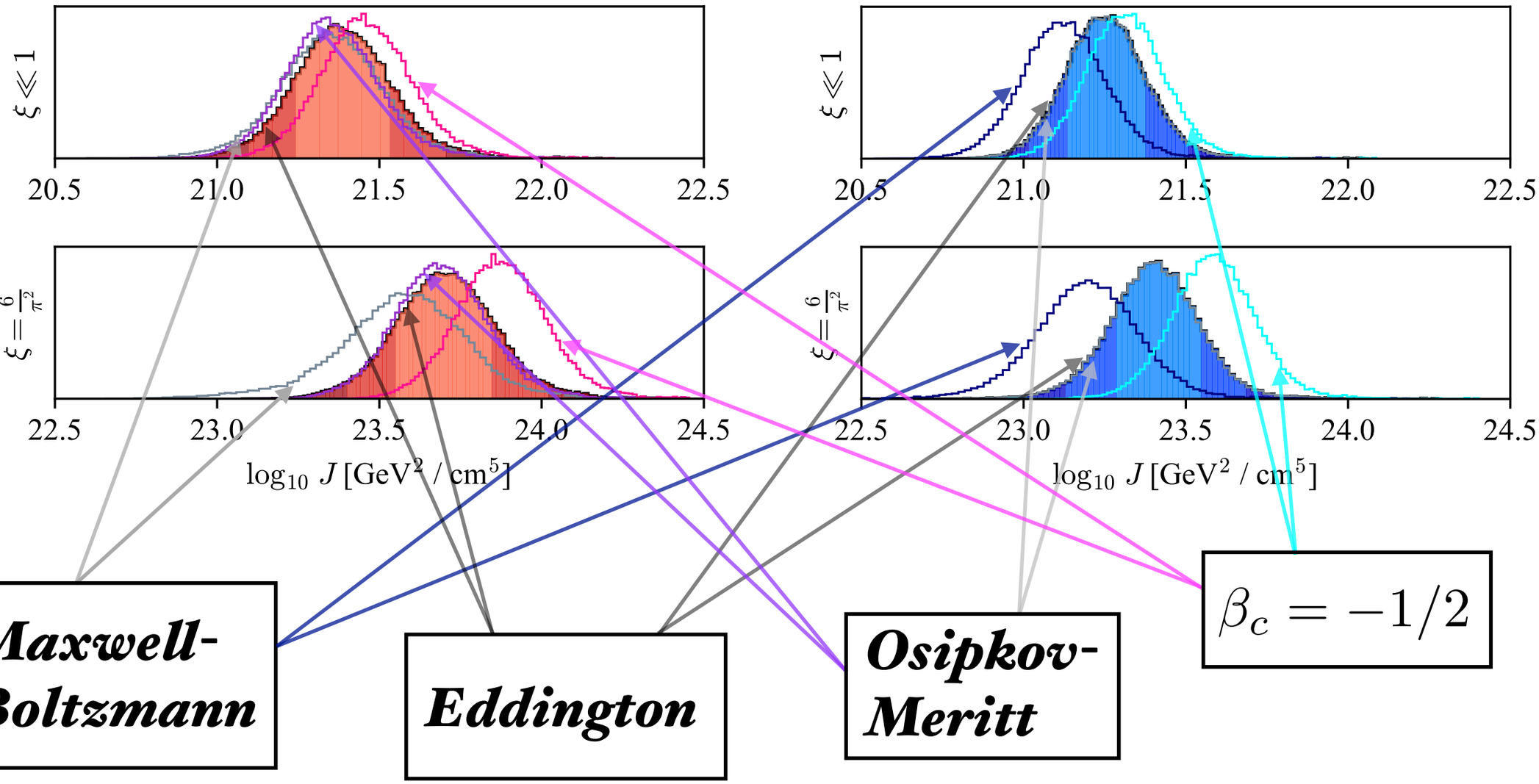

Petač, PU & Valli, 2018

J-factor summary results for the 8 classical dwarfs:

A significantly larger uncertainty than restraining to the approximate "radially-dependent" Maxwell-Boltzmann PSDF:

Coulomb regime

resonant regime

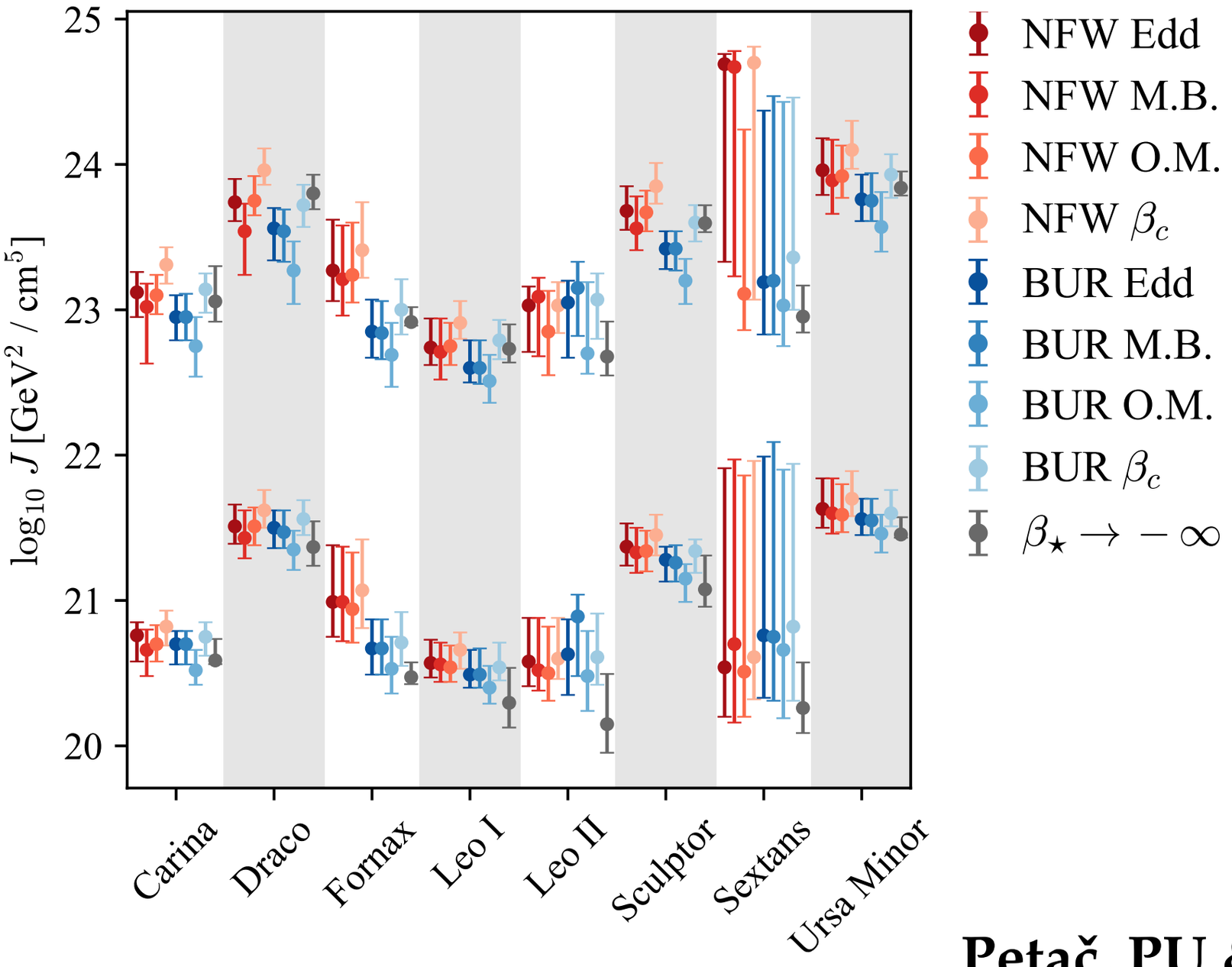

Petač, PU & Valli, 2018

Conclusion:

MW dwarf satellites are an ideal target for dark matter indirect detection, with the prompt emission of gamma-rays being a smoking-gun signature.

Null searches with the Fermi LAT have been interpreted as excluding thermal relic WIMPs lighter than about 100 GeV.

Some caution is needed, examining critically what are the assumptions involved in deriving such limits. The impact of an alternative mass model approach has been discussed here.

We have also discussed here - for the first time - the impact of different classes of phase space distribution functions on predictions for WIMP models with velocity dependent annihilation cross sections.